Electrolyzers in the System Advisor Model (SAM): A Techno-Economic Potential Study

William Xi, Matthew Boyd, Mark Ruth, and Parthiv Kurup

NREL is a national laboratory of the U.S. Department of Energy
Office of Energy Efficiency & Renewable Energy
Operated by the Alliance for Sustainable Energy, LLC

This report is available at no cost from the National Renewable Energy Laboratory (NREL) at www.nrel.gov/publications.

Contract No. DE-AC36-08GO28308

Technical Report
NREL/TP-6A20-83155
March 2023

Electrolyzers in the System Advisor Model (SAM): A Techno-Economic Potential Study

William Xi, Matthew Boyd, Mark Ruth, and Parthiv Kurup

Suggested Citation
Xi, William, Matthew Boyd, Mark Ruth, and Parthiv Kurup. 2023. *Electrolyzers in the System Advisor Model (SAM): A Techno-Economic Potential Study*. Golden, CO: National Renewable Energy Laboratory. NREL/TP-6A20-83155.
https://www.nrel.gov/docs/fy23osti/83155.pdf.

NREL is a national laboratory of the U.S. Department of Energy
Office of Energy Efficiency & Renewable Energy
Operated by the Alliance for Sustainable Energy, LLC

This report is available at no cost from the National Renewable Energy Laboratory (NREL) at www.nrel.gov/publications.

Contract No. DE-AC36-08GO28308

Technical Report
NREL/TP-6A20-83155
March 2023

National Renewable Energy Laboratory
15013 Denver West Parkway
Golden, CO 80401
303-275-3000 • www.nrel.gov

NOTICE

This work was authored by the National Renewable Energy Laboratory, operated by Alliance for Sustainable Energy, LLC, for the U.S. Department of Energy (DOE) under Contract No. DE-AC36-08GO28308. Funding provided by the U.S. Department of Energy Office of Energy Efficiency and Renewable Energy Hydrogen and Fuel Cells Technology Office and the U.S. Department of Energy Office of Energy Efficiency and Renewable Energy Solar Energy Technologies Office. The views expressed herein do not necessarily represent the views of the DOE or the U.S. Government.

This report is available at no cost from the National Renewable Energy Laboratory (NREL) at www.nrel.gov/publications.

U.S. Department of Energy (DOE) reports produced after 1991 and a growing number of pre-1991 documents are available free via www.OSTI.gov.

Cover Photos by Dennis Schroeder: (clockwise, left to right) NREL 51934, NREL 45897, NREL 42160, NREL 45891, NREL 48097, NREL 46526.

NREL prints on paper that contains recycled content.

Acknowledgements

The authors acknowledge the support we have received from many individuals in providing assistance with developing the framework and modeling efforts. Firstly, we acknowledge the Solar Energy Technologies Office and the Hydrogen and Fuel Cell Technologies Office who have supported this work with valuable insights and funding. In these offices, we would like to thank Vijaykumar Rajgopal and Katie Randolph for their guidance on modeling PV and concentrating solar technologies coupled with electrolytic hydrogen production and providing insights on assumptions used in developing the framework.

Secondly, we acknowledge the System Advisor (SAM) Model team at NREL who helped scope and layout our eventual framework for hydrogen analysis in the SAM environment. In particular, we would like to thank Nate Blair, Janine Keith, and Brian Mirletz. We would also like to acknowledge Kazunori Nagasawa at NREL for their support in modeling low temperature electrolyzers and rectifiers. In addition, we would like acknowledge colleagues at Idaho National Laboratory for providing a high temperature electrolyzer model for use in our framework; we especially appreciate the support provided by Dan Wendt in describing the HTSE modeling framework in ASPEN and providing critical data necessary to model the HTSE in our framework.

Finally, we would like to thank our reviewers: James Vickers, William Gibbons, Rajgopal Vijaykumar, Dan Bilello, Alex Badgett, and Janna Martinek for their valuable insights. Their suggestions greatly improved the quality and merit of this report.

List of Acronyms and Abbreviations

AC	alternative current
ATB	Annual Technology Baseline
BIL	Bipartisan Infrastructure Law
BOP	balance of plant
CAPEX	capital expenditures
CSP	concentrating solar power
DC	direct current
DOE	U.S. Department of Energy
FTE	full-time equivalent
GIS	geographic information system
H_2	hydrogen
H2A	hydrogen analysis
HLC	hydrogen levelized cost
HTF	heat transfer fluid
HTSE	high-temperature steam electrolyzer
HX	heat exchanger
HFTO	Hydrogen and Fuel Cell Technologies Office
HOPP	Hybrid Optimization and Performance Platform
INL	Idaho National Laboratory
IRA	Inflation Reduction Act
KNO_3	potassium nitrate
LHV	lower heating value
LMP	locational marginal prices
LTE	low-temperature electrolyzer
MACRS	Modified Accelerated Cost Recovery System
MSALT	molten salt
MW	megawatt
NE	Office of Nuclear Energy
NMC	nickel-manganese-cobalt
NO_3	nitrate
NOAK	n^{th} of a kind
NPV	net present value
NREL	National Renewable Energy Laboratory
OD	outer diameter
OPEX	operating expenditures
PEM	polymer electrolyte membrane
PV	photovoltaic
SAM	System Advisor Model
SMR	steam methane reforming
SNL	Sandia National Laboratories
SETO	Solar Energy Technologies Office
SOC	state of charge
TEA	techno-economic analysis
TRL	technology readiness level

Executive Summary

This report builds upon a growing body of work in the techno-economics of hydrogen production from renewable resources. Initiatives such as H2@Scale have been started to address the challenges developing hydrogen's potential role in the future energy system. Of particular interest is the concept of green hydrogen where hydrogen is produced with minimal CO_2 emissions. Over the last 100 years, hydrogen has been produced through steam methane reforming (SMR), which has CO_2 emissions and is often described as grey hydrogen. Out of the multitude of green hydrogen production pathways, solar to electrolytic hydrogen is of great interest due to increasing deployment of both photovoltaics and concentrating solar technologies. On the electrolytic hydrogen production side, polymer electrolyte membrane (PEM) electrolyzers and high temperature electrolysis (HTSE) are seeing growing interest due to load-following capabilities of PEM electrolyzers and higher efficiency HTSEs. A standardized framework that connects commonly used hydrogen analysis tools with solar modeling tools did not exist before this work.

In this report, we describe a framework that integrates the industry-standard solar modeling tool known as the System Advisor Model (SAM) and a commonly used hydrogen analysis tool known as H2A. The framework is developed in Python 3.8.8 using PySAM ("NREL-PySAM 3.0.1") to interface with the SAM code base. Electrolytic hydrogen production models are coded in Python. The default low-temperature electrolyzer (LTE) model in this framework is based on the H2A current and future centralized hydrogen production models (James 2013) . The default high-temperature steam electrolyzer (HTSE) model in this analysis is based on the HTSE model developed by Idaho National Laboratory INL) (Wendt and Knighton 2022). All solar models are based on existing SAM unit modules and can be created within the framework by initializing a PySAM unit module or by reading a Javascript object notation (JSON) file generated using the SAM desktop application. Material and energy flows from the solar models in PySAM and electrolyzer models are sent to a levelized cost calculator in either SAM or H2A to calculate hydrogen levelized costs (both options are available).

The framework described in this report integrates SAM with H2A electrolyzer technologies and provides analysts a detailed technoeconomic method to analyze concentrating and photovoltaic (PV) solar technologies to produce energy that are directly coupled to LTE and HTSEs that use that energy to split water into hydrogen and oxygen. This method is valuable in understanding potential impacts of performance, cost, and location on hydrogen levelized costs (HLCs). However, the analysis presented in this report does not include provisions in the Bipartisan Infrastructure Law (BIL) or the Inflation Reduction Act (IRA) such as production tax credits for either electricity or hydrogen. Subsequent analysis could include those provisions after they are finalized by the U.S. Treasury Department as well as estimates regarding how more developed markets could result in more mature manufacturing and supply chains and thus reduce the costs of solar and electrolysis equipment more rapidly than estimated in this analysis. As a result, this analysis is complementary to analyses used to set the U.S. Department of Energy (DOE) targets of $2/kg hydrogen by 2026 and $1/kg by 2031 because analysts can use this methodology to identify technical parameters and locations under which those goals can be achieved for tightly coupled solar-hydrogen systems and consider where other options (e.g., grid-connected and hybrid) systems could reduce HLCs. This methodology also provides analysts with the ability to estimate HLCs for opportunities where hydrogen is economically competitive before meeting DOE's targets.

The technoeconomics of four solar hydrogen systems are investigated using the framework that integrates SAM with H2A. The four systems are detailed in Table ES-1. The Four Hydrogen Production Systems Modeled using the H_2 in SAM Framework.

Table ES-1. The Four Hydrogen Production Systems Modeled using the H_2 in SAM Framework

System	Description
Grid-LTE	An LTE module connected to the grid that operates in response to grid electricity prices in a price-taker scenario.
PV-LTE With Optional Battery Storage	A PV farm coupled to an LTE module through an alternative current-direct current (AC-DC) connection with optional AC-connected battery storage ranging from 1 to 12 hours. The overall system is islanded with a small grid connection for parasitics.
MSALT-HTSE	A molten salt tower coupled to an HTSE module wherein the hybrid molten salt tower provides heat and electricity to the HTSE module. An auxiliary boiler and grid connection are used to handle HTSE hot standby and tower parasitics. Electricity and heat is assumed to be used within the system and cannot be exported or sold.
PV-MSALT-HTSE	A PV farm and heat-only molten salt tower coupled to an HTSE module wherein the PV farm provides electricity, and the tower provides heat to the HTSE module. An auxiliary boiler and grid connection are used to handle HTSE hot standby and tower parasitics. Electricity and heat is assumed to be used within the system and cannot be exported or sold.

Two scenarios are analyzed for each system: 2020 and 2050. Daggett, CA is the site location for both scenarios. An additional U.S.-wide analysis is conducted to highlight lowest cost solar to hydrogen production trends across the U.S. in both 2020 and 2050. The component size and operating strategy is varied for each hydrogen production system to identify the lowest cost system configuration and whether \$2/kg H_2 is achievable given system cost and performance estimates.

Table 2 below show the baseline system configurations and resulting HLCs for the 2020 and 2050 scenarios using this framework. In the 2020 scenario, no system achieves \$2/kg H_2. The lowest cost system in the 2020 scenario is the grid electrolysis system with the PV-MSALT-HTSE being the only solar hydrogen system that is competitive. In the 2050 scenario, PV-LTE and PV-MSALT-HTSE systems approach \$2 /kg H_2.

Table ES-2. Baseline System Configurations and the 2020 and 2050 Scenario Hydrogen Levelized Costs

System	System Capacities	HLC 2020 (2020$/kg H_2)	HLC 2050 (2020$/kg H_2)
Grid-LTE	131 MW LTE with $20 /MWh Price Adder to Locational Marginal Prices	2.82	2.50
PV-LTE	100 MW PV | 55 MW LTE	3.86	2.13
MSALT-HTSE	115 MWe/22 MWth Tower | 115 MW HTSE	3.93	2.84
PV-MSALT-HTSE	100 MW PV | 15 MWth Tower | 60 MW HTSE	2.90	2.15

To achieve the $2/kg H_2 target in locations with excellent solar resources such as Daggett, California, cost parameters similar to aggressive R&D targets will need to be achieved for all the systems analyzed. In Daggett, PV costs of $0.68 /Wac or moderate Annual Technology Baseline (ATB) PV capital expenditure (CAPEX) projections result in HLCs of $2 /kg H_2. Similarly for PV-MSALT-HTSE systems, $0.60 /Wac result in $2/kg H_2. Both cost requirements are similar ATB moderate R&D 2050 projections. For the MSALT-HTSE systems, better than aggressive 2050 ATB salt tower CAPEX projections would be needed to reach $2/kg H_2. Molten salt tower capital costs (includes the power block and thermal storage) of $2400/kW would enable $2/kg H_2 in 2050. That cost is slightly lower than current advanced ATB R&D projections of $2,743/kW in 2050. Outside of Daggett and other excellent solar resource locations, it is unlikely that $2/kg H_2 is obtainable using current 2050 cost projections.

A U.S.-wide analysis is conducted by sizing and calculating the HLC for all four systems at locations where centralized hydrogen production plants could potentially be built. The locations are selected based primarily on proximity to hydrogen related infrastructure and covering the range of solar resource levels in the U.S. This analysis is conducted for both the 2020 and 2050 scenarios to compare the cost of producing hydrogen for all systems and to identify changes in the relative HLCs between systems moving from the 2020 to 2050 scenarios. Figure ES-1 below shows the PV-LTE system has the lowest HLC across all 40 locations in the continental U.S. in the 2050 scenario. However, PV-LTE systems only achieve near $2/kg H_2 HLCs in locations with excellent solar resources such as New Mexico, Arizona, and Southern California. In other locations, HLCs for the lowest cost hydrogen production systems generally range from $2.5 to 4/kg H_2.

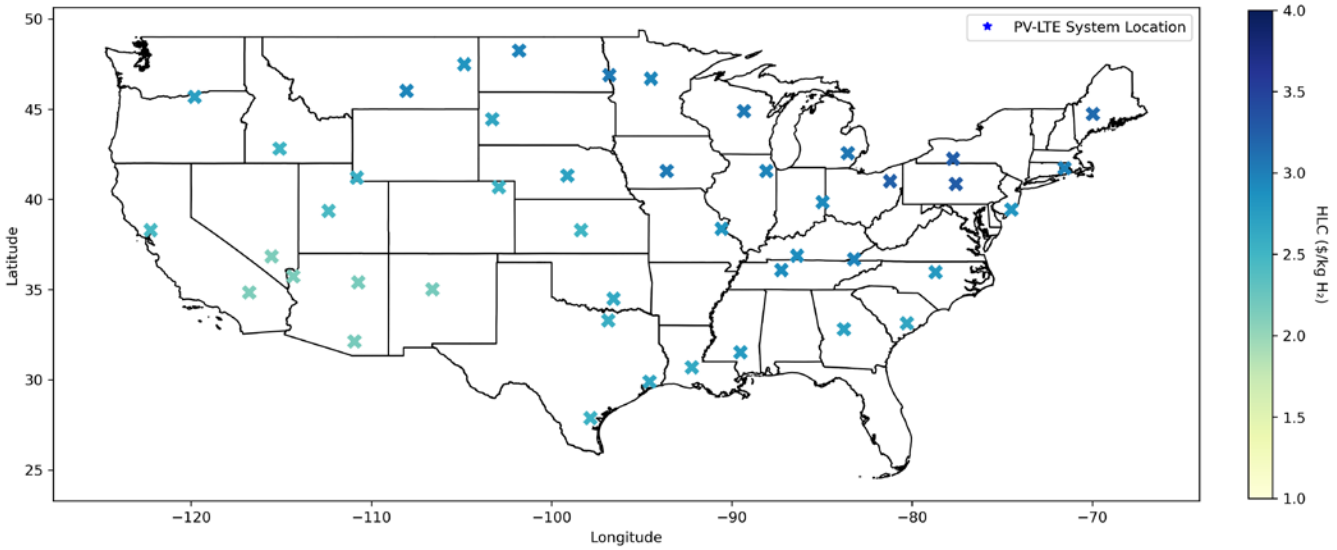

Figure ES-1. Lowest Cost Hydrogen Production Systems in the 2050 Scenario Across 40 Locations in the U.S.

The U.S. wide analysis also highlighted several other trends. PV-MSALT-HTSE HLCs in the 2050 scenario are within 1% of PV-LTE system HLCs in locations with excellent solar resources. Thus, PV-MSALT-HTSE systems could be a pathway to lower cost hydrogen production in locations where it would be feasible to produce hydrogen from solar competitively. While PV-MSALT-HTSE systems remain cost competitive among the four systems in both scenarios, this analysis indicates PV-LTE systems are the most likely system to achieve \$2/kg H_2 outside of the southwestern U.S. Analysis using the advanced R&D ATB scenario PV capital costs result in PV-LTE systems in the Midwest achieving \$2/kg H_2. However, PV-MSALT-HTSE systems do not achieve \$2/kg H_2 HLC without additional cost reductions beyond current 2050 estimates (e.g., molten salt tower costs). Lastly, the HLC of PV-LTE systems can be further reduced by operating a smaller electrolyzer for a 100 MW PV system at a higher capacity factor using battery storage. Given the DOE Earthshot, Long Duration Storage Shot target of a 90% reduction in current 2020 Li-ion battery capital costs, HLCs of PV-LTE systems with utility battery scale storage can be competitive or noticeably lower than the HLCs of PV-LTE systems without batteries.

Table of Contents

List of Figures

List of Tables

1 Introduction

In the United States, hydrogen (H_2) is used in oil refining for hydrotreating and desulfurization; is a key intermediate in ammonia production; has applications in industrial processes, including liquid fuel production; and is a potential direct fuel for light- and heavy-duty vehicles. With these wide-ranging applications and the potential to expand H_2 usage as a renewable source of energy, an interest has arisen in finding alternatives to the current state-of-the-art method for H_2 production—steam methane reforming (SMR)—that are less carbon-intensive. A viable alternative to the SMR process would be cost-competitive while avoiding the greenhouse gas emissions inherent in SMR.

An effort aligned with these clean hydrogen production goals, the "Concentrated Solar Power as a Pathway for Electrolytic Hydrogen Production Project" is a U.S. Department of Energy Hydrogen and Fuel Cell Technologies Office (DOE-HFTO) and U.S. Department of Energy Solar Energy Technologies Office (DOE-SETO) joint-funded project. This initiative aims to identify parameter spaces where electrolytic hydrogen production using concentrated solar power (CSP) technologies can approach U.S. Department of Energy (DOE) hydrogen levelized costs (HLCs) of $2 per kilogram ($2/kg) H_2, with a pathway to $1/kg H_2, as per the Hydrogen Shot goals in the DOE Energy Earthshot, Hydrogen Shot framework ("DOE Energy Earthshots - Hydrogen Shot" 2021). To achieve this objective, our project team developed a tool that connects low-temperature electrolyzer (LTE) and high-temperature electrolyzer (HTSE) models to the industry-standard System Advisor Model (SAM) solar simulation software.

LTE, which uses electricity to split water into hydrogen and oxygen, can run on grid or photovoltaic (PV) electricity; HTSE uses both heat and electricity to split water. Although HTSE is considered more efficient than LTE and could have a lower cost, this process requires stable, high-temperature heat input. CSP with molten salt solar power towers is a potential option to provide the HTSE process with its heat and electricity requirements. Hybrid CSP heat and PV electricity could also be a step toward lower-cost hydrogen production from the benefits of lower-cost PV electricity and the availability of heat from CSP. As described in this report, the modeling tool developed by our project team can be used to analyze multiple hydrogen production systems. By using the tool developed by our project team, both hydrogen and CSP researchers can conduct CSP-to-hydrogen techno-economic analysis (TEA).

The framework described in this report integrates SAM with H2A electrolyzer technologies and provides analysts a detailed technoeconomic method to analyze concentrating and photovoltaic solar technologies to produce energy that are directly coupled to LTE and HTSEs that use that energy to split water into hydrogen and oxygen. This method is valuable in understanding potential impacts of performance, cost, and location on HLCs. However, the analysis presented in this report does not include provisions in the Bipartisan Infrastructure Law (BIL) or the Inflation Reduction Act (IRA) such as production tax credits for either electricity or hydrogen. Subsequent analysis could include those provisions after they are finalized by the U.S. Treasury Department as well as estimates regarding how more developed markets could result in more mature manufacturing and supply chains and thus reduce the costs of solar and electrolysis equipment more rapidly than estimated in this analysis. As a result, this analysis is complementary to analyses used to set the U.S. Department of Energy (DOE) targets of $2/kg hydrogen by 2026 and $1/kg by 2031 because analysts can use this methodology to identify technical parameters and locations under which those goals can be achieved for tightly coupled solar-hydrogen systems and consider where other options (e.g., grid-connected and hybrid) systems could

reduce HLCs. This methodology also provides analysts with the ability to estimate HLCs for opportunities where hydrogen is economically competitive before meeting DOE's targets.

After providing background on the tool development and scope, including the models developed in SAM to calculate hydrogen production, this report describes the four hydrogen production systems that were constructed for analysis in our study: Grid-LTE, PV-LTE (PV coupled to LTEs with optional battery storage), MSALT-HTSE (molten salt tower coupled to an HTSE module), and PV-MSALT-HTSE (PV farm and heat-only molten salt tower coupled to an HTSE module). Finally, we discuss the techno-economics of the CSP-to-hydrogen systems that were created. These techno-economics are compared to baseline PV-to-hydrogen systems and grid electrolysis.

1.1 H2@Scale and Centralized Solar-to-Hydrogen Pathways

The H2@Scale initiative is helping to enable decarbonization across industrial sectors by advancing hydrogen in efforts from production to storage and grid resiliency (Pivovar, Rustagi, and Satyapal 2018). Figure 1 illustrates the landscape of hydrogen production and use in the United States, as well as its links to the electric grid infrastructure. H2@Scale looks at hydrogen as a clean energy carrier. Hydrogen is used to convert energy from the electrical grid for use in various applications such as fuel cell electric vehicles, biomass upgrading and metal refining. A major obstacle to the widespread adoption of green hydrogen is the lack of a cost-competitive production route via renewables. With renewable energy such solar growing rapidly, understanding the techno-economics of various solar to hydrogen systems is critical to identifying cost-competitive pathways for centralized hydrogen production. This initial tool developed by the project team seeks to provide hydrogen analysts a method to identify cost-competitive solar to hydrogen systems, ultimately providing insight into how such systems may fit within the H2@scale vision.

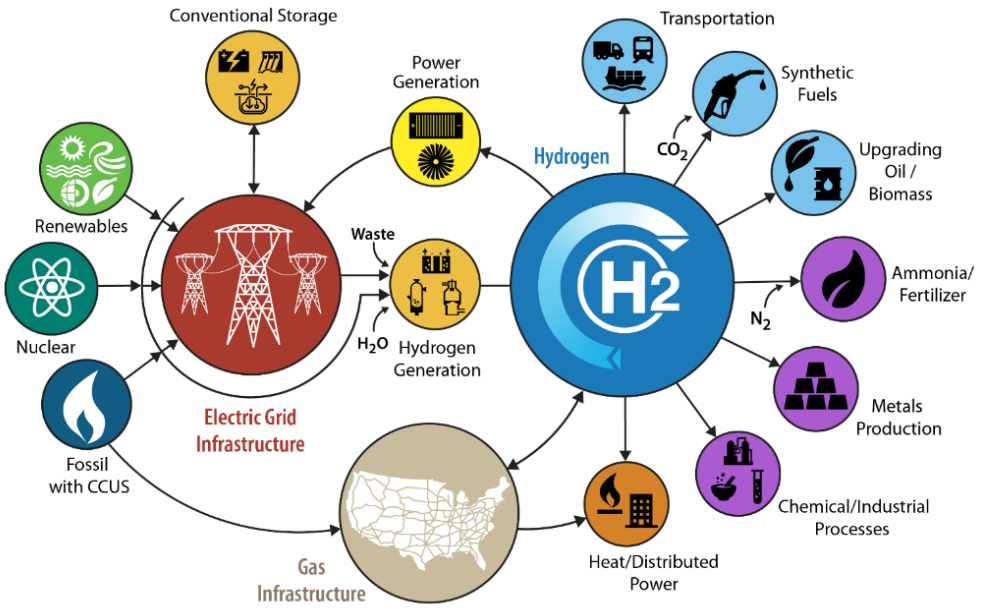

Figure 1. Schematic Illustrating an Integrated Hydrogen Energy System in H2@Scale (Pivovar, Rustagi, and Satyapal 2018)

In addition, as a part of the solar-hydrogen TEA in this report, a United States-wide analysis involving 40 selected locations and all systems was conducted. Using current (2020) and future (2050) cost and performance assumptions, the technoeconomic analysis provides insight into the lowest cost hydrogen production systems in both scenarios, cost and performance targets that enable competitive hydrogen levelized costs, and when a broader category of locations within the United States can achieve \$2/kg H_2.

1.2 Hydrogen Analysis in SAM

Historically, solar modeling tools (e.g., SAM) and hydrogen production modeling tools (e.g., H2A) have been available and seen widespread use in energy analysis. The H2A production models are discounted cash flow models that use consistent process design assumptions and cost analysis methodology to analyze various hydrogen production systems. SAM is techno-economic software model for renewable energy systems to facilitate decision making for the renewable energy industry. However, no preceding effort has combined these two types of modeling tools to develop a hybrid, solar-to-hydrogen analysis tool. The tool developed during this project is an extension of an industry-standard tool to enhance its usage. With the ability to analyze multiple scenarios through the integration of LTE and HTSE models into SAM, steps can be taken to identify pathways to \$2/kg H_2, and eventually \$1/kg H_2. Because LTE and HTSE electrolyzer technologies are being adopted more frequently and with greater interest, there is a door open to expand the existing work on understanding the various benefits of different solar to hydrogen systems. The tool developed in this project provides a starting point for developing and analyzing a multitude of validated solar technology models and electrolyzer combinations. Section 3 of this report provides some examples of the technoeconomic analysis work that can be done within this tool.

This report concludes with a discussion of our findings regarding whether solar H_2 systems can be competitive with Grid-LTE and/or SMR systems. The systems that can achieve \$2/kg H_2 are discussed along with the cost reductions needed to make that achievement in Daggett, California, our primary basis location for analysis. The impact of battery storage on reducing the overall HLCs of PV-LTE systems is also reviewed.

2 Methods

2.1 Hydrogen Analysis in SAM Architecture

The architecture for the overall tool created in this study uses Python 3.8.8 with the PySAM ("NREL-PySAM 3.0.1") wrapper for SAM, as shown in Figure 2. This structure is used to link existing SAM capabilities for PV solar, CSP, and CSP heating technologies with the LTE and HTSE modules, which were developed in Python 3.8.8.

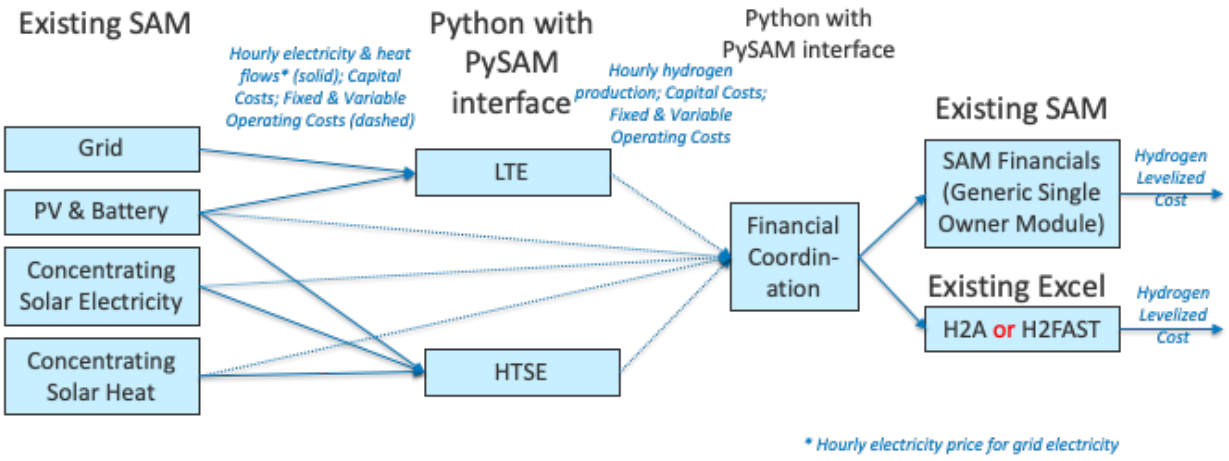

Figure 2. Overall structure for SAM integrated with LTE and HTSE models

Using the tool, analyses are performed on an hourly basis to account for hourly data sources, such as electricity prices and the default SAM resolution. The SAM models transfer data to the LTE and HTSE modules, including hourly electricity and heat flows, capital and operating costs, and miscellaneous parameters such as parasitic loads and battery lifetimes. Hourly grid electricity prices from existing published locational marginal prices are transferred to the LTE and HTSE Python modules.

The LTE and HTSE modules use electrical energy inputs and efficiencies to calculate hydrogen production, and the HTSE module also uses heat energy inputs in its calculations. A financial coordination module then takes the capital, fixed, and variable operating costs for the solar-hydrogen systems, as well as hourly hydrogen production rates from the LTE and HTSE modules, to determine the HLCs. The role of the financial coordination module is to send performance and financial results to both the existing SAM financial calculator and H2A or H2FAST ("H2FAST: Hydrogen Financial Analysis Scenario Tool" 2017) so that the HLC and other financial results can be generated with the user's preferred tool.

PySAM does have limitations that will be discussed in detail in the individual sections below. The SAM models can be difficult to customize, while feedback from the electrolyzer models to the SAM modules is not currently implemented. In addition, this work will not be incorporated into the SAM graphical user interface. Using Python, however, allows for quicker development and adjustments of the electrolyzer system models and integration with SAM compared to developing the models in the SAM source code. The code is available as a standalone GitHub repository under NREL at https://github.nrel.gov/wxi/sam-electrolysis.

2.2 Low Temperature Electrolyzer Modeling (PEM)

Two LTE performance models were used for this analysis: a constant hydrogen production efficiency model based on H2A and a performance curve model. The H2A hydrogen production model was selected as the default model as it is an industry vetted hydrogen production model used in a multitude of hydrogen analysis work done at NREL. Thus, having a consistent set of assumptions from H2A allows for meaningful comparison of technoeconomic analyses using this tool with other work in this research area. A performance curve model is also implemented to allow researchers to cover PEM stack performance models that result from theoretical analysis or experimental data. As described in this

section, the performance curve model is generic and typically requires an input that relates stack power consumption to current.

Constant Efficiency Model

The constant efficiency model based on H2A assumptions distributes power input between the stack and balance of plant (BOP) to determine the hydrogen production rate. The constant efficiency model assumptions are presented in Table 1.

Table 1. LTE Constant Hydrogen Production Efficiency Model Assumptions

PEM Electrolysis System	H_2 Production Efficiency Stack (kWhDC/kg H_2)	Voltage Efficiency (% LHV)	Current Density (mA/cm^2)	Replacement Frequency (years)	Replacement Cost (% of installed)	BOP Load (kWhAC/ kg H_2) [a]
H2A (Current Central)	50.4 @ 80°C	65.9 @ 80°C	2,000 @ 80°C	7	0.15	2.45
H2A (Future Central)	47.8 @ 80°C	69.6 @ 80°C	3,000 @ 80°C	10	0.12	2.1

PEM = Polymer electrolyte membrane

kWhDC/kg H_2 = Kilowatt-hours direct current per kilogram hydrogen

LHV = Lower heating value

mA/cm^2 = Milliampere per square centimeter

kWhAC/kg H_2 = Kilowatt-hours alternating current per kilogram hydrogen

[a] H2A accounts for rectifier loss to convert AC power to DC power in the BOP load (stack eff/η_{rect} – stack eff is the contributing component). Because we use a separate rectifier model, we assume the DC power input into the stack remains the same and account for the variable rectifier loss separately.

The power distribution between the BOP and the stack is solved using a generic root finder, which solves for a split fraction such that the electricity balance between the stack and BOP converges for each hour. At each hour, the electricity balance across the electrolyzer system is calculated as shown in Equation (1) where $P_{AC,Stacks,t}$ and $P_{AC,BOP,t}$ is the actual AC electricity used by the stack and BOP at a given hour t.

$$P_{AC,t} = P_{AC,Stacks,t} + P_{AC,BOP,t} \quad (1)$$

The balance of plant power input is assumed to be a linear function of the hydrogen production rate. However, in practice there are electricity losses in the system and hours where there is excess electricity that the electrolyzer cannot use. Thus, Equation (1) is expanded to include cases where the input power to the stack is too low (i.e., below 5% of the stack rating) and when the electricity exceeds the combined nominal capacity of the number of parallel stacks specified. The energy balance across all of the stacks is thus defined as indicated in Equation (2).

$$P_{AC,t} = P_{AC,Stacks,t} + P_{AC,BOP,t} + P_{AC,Rect,t} + P_{AC,Excess,u,t} + P_{AC,Excess,l,t} \quad (2)$$

where $P_{AC,Excess,u,t}$ is curtailed electricity beyond the nominal capacity of the electrolyzer (see Equation (3)) and $P_{AC,Excess,l,t}$ represents curtailed electricity due to lower operating limits of the electrolyzer (see Equation (4)).

$$P_{AC,t} - (Capacity_{DC} / \eta_{rect,nom} * n_{rows}) - P_{AC,BOP,nom} > 0 \quad (3)$$

where $Capacity_{DC}$ is the nominal DC capacity for a single stack, $\eta_{rect,nom}$ is the nominal rectifier efficiency, n_{rows} is the number of electrolyzer stacks arranged in parallel, and $P_{AC,BOP,nom}$ is the nominal BOP load associated with the nominal stack DC capacity. In other words, this term represents when the available energy to the electrolyzer is greater than its nominal load.

The $P_{AC,Excess,l,t}$ is described by Equation (4).

$$\Sigma P_{AC,i,t} \text{ if } P_{AC,i,t} * \eta_{rect,t} < min_{load} * Capacity_{nomDC} \ \forall \ i \in stacks \quad (4)$$

where $P_{AC,i,t}$ represents the individual power sent towards an individual stack if multiple stacks are arranged in parallel. In a single stack system, $P_{AC,i,t}$ would be equivalent to $P_{AC,Stacks,t}$. In the case of a parallel stack configuration, power is distributed such that as many stacks receive a nominal power input as possible. This term represents when the available energy is below the minimum operating load of the electrolyzer. This minimum load is enforced to represent potential safety concerns with the impact of gas crossover at lower loads or to represent a general turndown ratio for an electrolyzer . With the power input into the stack balanced, the following calculations are conducted to determine hourly stack outputs for the analysis period Y (years). The stack is assumed to produce hydrogen at a constant efficiency for all hours in the year as per the H2A production models.

The hydrogen production rate across all stacks is described by Equation (5).

$$H_{2,out,t} = P_{AC,Stacks} * \eta_{rect,t} / H_{2,eff} \ \forall \ t = 1..Y*8760 \quad (5)$$

$H_{2,eff}$ represents the amount of electrical energy required to produce a kg of hydrogen or in other words the hydrogen production efficiency. This value depends on the H2A scenario. The process waterflow rate is defined by Equation (6).

$$H_2O_t = 3.78 \text{ (gal/kg } H_2) * H_{2,out,t} \ \forall \ t = 1..Y*8760 \quad (6)$$

Performance Curve Model

The performance curve model is based on variations of an I-V curve, as show in Figure 3. The model formulation is presented below after the figure. The performance curve model requires a stack performance curve that determines the stack current for a given stack power input and temperature for a specified nominal stack rating as an input. The stack pressure and the pressure of the hydrogen produced are assumed to be equivalent to H2A assumptions. If no performance curve is specified, the default curve is based on experiments done on a Giner 225 kW stack at NREL. In addition, the balance of plant consumption is specified using a kg H_2/hr basis. The default BOP energy consumption per kg H_2/hr is based on H2A values.

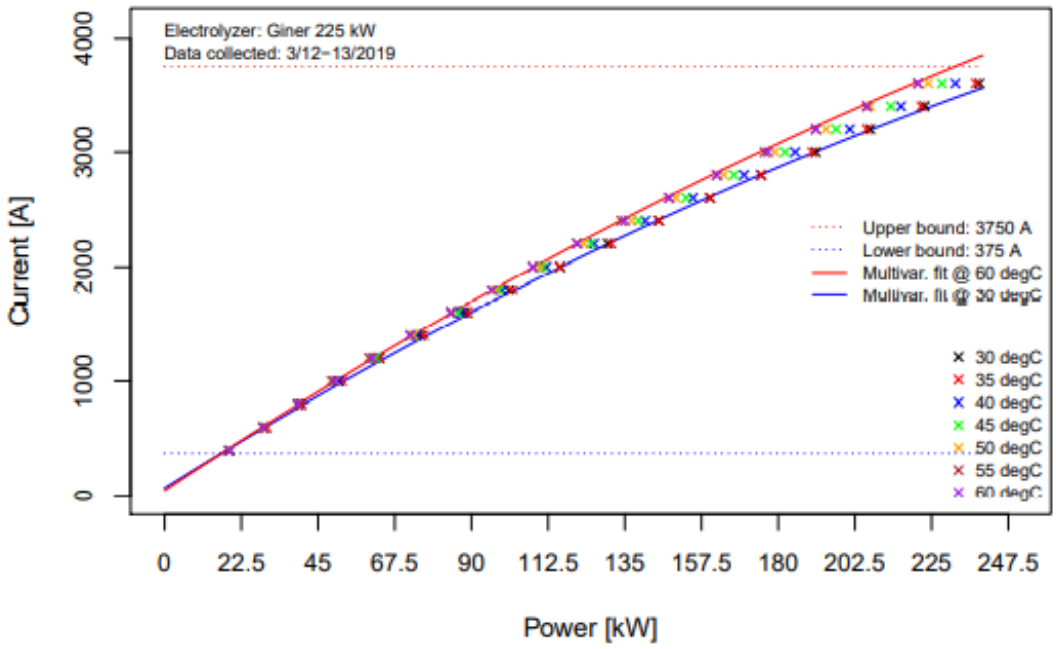

Figure 3. A Giner 225 kW PEM electrolyzer performance curve that relates current to power input and temperature

The cell active area and number of cells in a series per stack are also specified to calculate the current density and the cell voltage as a function of time, respectively. The Faraday efficiency of the system is defined as shown in Equation (7).

$$\eta_{f,i,t} = f(P_{AC,i,t} * \eta_{rect,t} \ / \ Capacity_{DC}) \ \forall \ i \in stacks \qquad (7)$$

where $P_{AC,i,t}$ represents the actual AC power input into a stack, $\eta_{rect,t}$ represents the rectifier efficiency and $Capacity_{DC}$ is the nominal DC rating of the electrolyzer stack. The default Faradaic efficiency curve is shown in Figure 4**.**

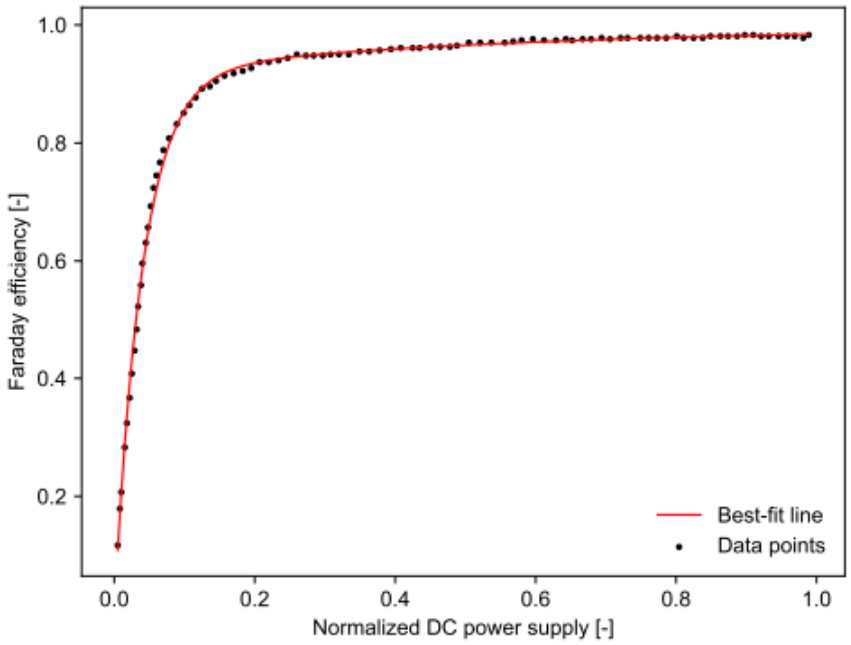

Figure 4. Faradaic efficiency curve as a function of the normalized DC power supply (Kotowicz, Węcel, and Jurczyk 2018)

Thus, given a power input ($P_{AC,i,t}$) and an optional hourly temperature input; a performance curve (I = f[P, T]); the cell active area (cm^2); and the number of cells, the following calculations are made to estimate the hydrogen production rate at each hour (t).

The stack current is calculated by using the stack performance curve described by Equation (8) where $I_{i,t}$ is the stack current at hour t .

$$I_{i,t} = f(P_{AC,i,t}, T_{t-1}) \quad \forall\, i \in \text{stacks} \tag{8}$$

The current density is calculated using the cell active area described by Equation (9) where A_{cell} is cell active area .

$$I_{density,t} = I_{i,t} / A_{cell} \quad \forall\, i \in \text{stacks} \tag{9}$$

The cell voltage is assumed to be the same across all cells and is described by Equation (10) where n_{cells} is the number of cells in series in the stack.

$$V_{cell,t} = V_{i,t} / n_{cells} \quad \forall\, i \in \text{stacks} \tag{10}$$

The hydrogen production rate is calculated using Faraday's law, as described by Equation (11).

$$H_{2,out,t} = I_{i,t} * M * \eta_{f,i,t} * c/(nF) \tag{11}$$

where M is the molar mass of hydrogen, c is the number of cells, n is the number of electrons per hydrogen molecule and F is Faraday's constant. Faraday's constant is 96485 A/mol, n is 2 and M is 2.016 g/mol H_2 respectively. The default LTE costs used are reported in Table 2 and Table 3 are based on H2A current and future central models. Note that the stack purchase cost generally varied in the scenarios analyzed.

Table 2. LTE Capital Costs

Stack Purchase Cost ($/kWDCStack)	BOP Mechanical, Electrical ($/kWDCStack)	Installation Factor	Indirect Costs (% Direct)			
			Site Preparation	Permitting	Contingency	Engineering /Design
143 (Future) 342 (Current)	23, 68 (Future) 36, 82 (Current)	1.10 (Future) 1.12 (Current)	2%	15%	15%	10%

$/kWDCStack = Dollar per kW of nominal stack capacity

Table 3. LTE Operating Costs

Plant Labor Cost	Overhead	Property Tax and Insurance	Material for Maintenance	Variable OPEX
$50/Hour	20% of Labor	2% of Total Capital Cost	3% of Direct Capital Cost	Cooling Water

The LTE CAPEX and OPEX calculations are presented below in the following equation. The overnight capital cost is described by Equation (12).

$$CAPEX_{overnight} = LTE_{nomcap} * (LTE_{CAPEX} * i_{install} * i_{indirect} + BOP_{mech,CAPEX} * i_{indirect} + BOP_{elec,CAPEX} * i_{indirect} * i_{install}) \quad (12)$$

where LTE_{nomcap} is the nominal capacity of the stack, LTE_{CAPEX} is the stack purchase cost, $i_{install}$ is the installation factor, $i_{indirect}$ is the total indirect cost factor, $BOP_{mech,CAPEX}$ is the mechanical BOP cost (including an inherent 46% installation factor), and $BOP_{elec,CAPEX}$ is the electrical BOP cost.

The operating costs for a given year (y) over the analysis period (Y) are described by Equation (13).

$$OPEX = labor + M\&R + PT\&I + R_{unplanned} + R_{planned} + O\&M_{variable} \quad (13)$$

where labor represents the labor costs for the centralized facilities, M&R represents the maintenance and repair costs, PT&I represents the property tax and insurance costs, $R_{unplanned}$ and $R_{planned}$ represents the unplanned and planned replacement costs and $O\&M_{variable}$ represents the variable operating and maintenance costs.

Labor costs are calculated using Equation (14) below where FTE is full time equivalent hours and overhead represents any overhead costs associated with labor.

$$\text{Labor} = 2080 \text{ hr/yr/FTE} * 50 (\$/\text{hr}) * 10 (\text{FTE}) * (1+\text{Overhead}) \quad (14)$$

Maintenance and repair costs are calculated using Equation (15) below where $CAPEX_{overnight}$ is the overnight capital cost and $i_{indirect}$ is the indirect cost multiplier.

$$M\&R = 0.03 * CAPEX_{overnight} / i_{indirect} \quad (15)$$

Property tax and insurance costs are calculated using Equation (16) below.

$$PT\&I = 0.02 * CAPEX_{overnight} \quad (16)$$

Unplanned replacement costs are calculated using Equation (17) below.

$$R_{unplanned} = 0.005 * CAPEX_{overnight} \quad (17)$$

Planned replacement costs are calculated using Equation (18) below where R_{frac} is the fraction of installed costs that represents replacement costs and R_{freq} is the frequency of the replacement cost.

$$R_{planned} = R_{frac} * CAPEX_{overnight}/i_{indirect} \text{ if } y \bmod R_{freq} = 0 \ \forall \ y = 1..Y \quad (18)$$

Variable O&M costs are calculated using Equation (19) below where $H_{2,out,y}$ is the annual hydrogen production rate in year y.

$$O\&M_{variable} = 0.002375 * H_{2,out,y} \ \forall \ y = 1..Y \quad (19)$$

An experimental DC power supply efficiency curve for a 750 kW stack tested at NREL is shown in Figure 5.

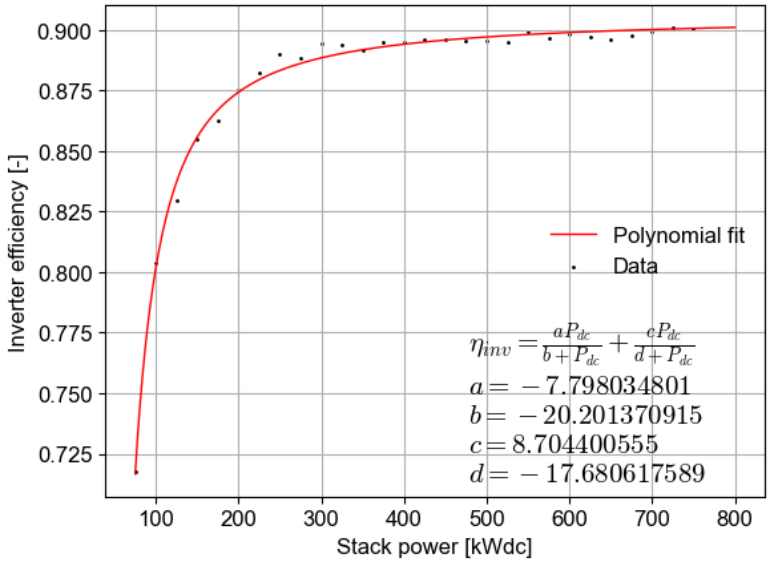

Figure 5. Rectifier efficiency curve

To apply this curve for a generic AC power provided by the grid or solar energy, we transform the domain of the plot by first normalizing the power input relative to the nominal stack capacity of 750 kW. We assume that by normalizing this stack, it can represent the single or multi-MW unit modules that comprise a centralized electrolytic hydrogen production facility. We then transform the normalized DC power to normalized AC power by using the rectifier efficiency. Thus, the inverter efficiency is now a function of normalized AC power input. The overall experimental curve is not defined entirely between zero and the nominal stack power input of 750 kW. To handle the missing data for the lower boundary, we assume rectifier efficiencies at normalized AC powers < 0.07 are equivalent to the efficiency at a normalized AC power of 0.07.

2.3 High Temperature Electrolyzer Modeling

The HTSE module is based on an Idaho National Laboratory (INL) model that was used on a project funded by the Office of Nuclear Energy (NE) in partnership with Xcel Energy Inc. The key modifications for this model are listed as follows:

1. The HTSE design is based on heat available at 300°C, and the cost and efficiency are unlikely to change significantly for heat sources between 250°C and 750°C.[1]
2. We assume 0% hydrogen loss during drying.
3. The model originally outputs hydrogen at 1,000 psi. The final stage in the multistage compressor is adjusted to produce hydrogen at 300 psi in alignment with the LTE model.
4. The hydrogen production rate for any load is determined by a linear interpolation between standby thermal and electrical efficiencies to full operating thermal and electrical efficiencies for 0% to 100% production. The interpolation equations are described by Equations 20–22.

   Min($H_{2,heat}$, $H_{2,elec}$), where:

[1] Dan Wendt (INL), Private Communication, February 12th 2021.

$$H_{2,heat} = (Q_t - Q_{stdby,frac} * Q_{nominal})/[(1- Q_{stdby,frac})*Q_{nominal}] * H_{2,nominal} \quad (20)$$

$$H_{2,elec} = (P_t - P_{stdby,frac} * P_{nominal})/[(1- P_{stdby,frac})*P_{nominal}] * H_{2,nominal} \quad (21)$$

$$Q_{nominal} = Heat_{eff}/Elec_{eff} * P_{nominal} \quad (22)$$

where $P_{nominal}$ is the nominal system power, $Q_{nominal}$ is the heat input at nominal system power, $Heat_{eff}$ and $Elec_{eff}$ are the thermal and electrical hydrogen production efficiencies at nominal system power, Q_{stdby_frac} and P_{stdby_frac} are the fraction of nominal thermal and electrical load required at hot standby, Q_t and P_t are the heat and power inputs at hour t, and $H_{2,nominal}$ is the nominal hydrogen production rate. Electrical and thermal energy must be provided in proportion, so we assume excess energy is curtailed. The HTSE performance assumptions are presented in Table 4.

Table 4. INL HTSE model performance assumptions

Scenario	Stack Operating Temperature	Stack Operating Pressure	Cell Voltage	Current Density	H_2 Purity	H_2 Product Pressure	Stack Replacement Frequency
Current	800^{O}C	5 Bar	1.285 V	1.0 A/cm^2	99.9 mol%	300 psi/20 bar	4 years
Future	800^{O}C	5 Bar	1.285 V	1.2 A/cm^2	99.9 mol%	300 psi/20 bar	7 years

System Electrical Efficiency @ Nominal Load (kWh/kg H_2)[a]	System Heat Efficiency @ Nominal Load (kWhth/kg H_2)	Electrical Efficiency @ Standby	Heat Efficiency @ Standby	Efficiency @ Intermediate Load	Heat Input Temperature (°C)	Electrical BOP Efficiency (kWhe/kg H_2)
36.801	6.40	0.9% Nominal	19% Nominal	Linear Interpolation	250	2.56

$/kWDCStack = Dollar per kW of nominal stack capacity

[a] Removal of 0.63 kWhe/kg H_2 by removing work streams associated with product compression in INL's Aspen HYSYS HTSE model

Given hourly power and heat inputs P (AC power) and Q, along with analysis period Y (years), the summarized calculation procedure for an hour t, ∀ t = 1..(Y*8760), is presented below. The nominal heat input to the stack is calculated using Equation (22). Excess heat ($Q_{excess,t}$) and electricity ($P_{excess,t}$) into the HTSE system are described by Equation (23) and Equation (24).

$$Q_{excess,t} = Q_t - Q_{nominal} \tag{23}$$

$$P_{excess,t} = P_t - P_{nominal} \tag{24}$$

The additional power ($P_{standby}$) and heat ($Q_{standby}$) required from the grid and boiler to meet electrolyzer hot standby loads are calculated using Equations (25) and Equation (26).

$$Q_{boiler} = -(Q_t - Q_{standby}) \text{ if } Q_t - Q_{standby} < 0 \text{ else } 0$$
$$\text{where } Q_{standby} = Q_{stdby,frac} * Q_{nominal} \tag{25}$$

$$P_{grid} = -(P_t - P_{standby}) \text{ if } P_t - P_{standby} < 0 \text{ else } 0$$
$$\text{where } P_{standby} = P_{stdby,frac} * P_{nominal} \tag{26}$$

The nominal hydrogen production rate based on input power and heat is calculated using Equation (27).

$$H_{2,nominal} = P_{nominal} / Elec_{eff} \tag{27}$$

The hydrogen production rate at a given hour (t) is the minimum of the two hydrogen production rates where $H_{2,out,t}$ is the hourly hydrogen production rate at hour t for the electrolyzer, $H_{2,heat,t}$ is the hydrogen production rate assuming heat is the limiting energy input and $H_{2,elec,t}$ is the hydrogen production rate assuming electricity is the limiting energy input.

$$H_{2,out,t} = \min(H_{2,heat,t}, H_{2,elec,t}) \tag{28}$$

The excess heat or electricity caused by imbalances in the ratio of heat to electricity at a given time t is calculated using the sequence described by Equation (29) to Equation (33).

If $H_{2,elec,t} < H_{2,heat,t}$:

Calculate the partial load condition of electricity (limiting resource) defined by P_{frac} using Equation (29):

$$P_{frac} = (P_t - P_{stdby,frac} * P_{nominal})/((1- P_{stdby,frac})*P_{nominal}) \quad (29)$$

Solve for the required heat input at this given partial load condition defined by $Q_{bal,t}$ using Equation (30):

$$Q_{bal,t} = P_{frac} *((1- Q_{stdby,frac})*Q_{nominal}) + Q_{stdby,frac} * Q_{nominal} \quad (30)$$

Determine the excess heat caused by imbalance in energy inputs defined by $Q_{excess,bal,t}$ using Equation (31):

$$Q_{excess,bal,t} = Q_t - Q_{t,bal} \quad (31)$$

If $H_{2,heat,t} < H_{2,elec,t}$:

Calculate the partial load condition of heat (limiting resource) defined by Q_{frac} using Equation (32):

$$Q_{frac} = (Q_t - Q_{stdby,frac} * Q_{nominal})/((1- Q_{stdby,frac})*Q_{nominal}) \quad (32)$$

Solve for the required power input at this given partial load condition defined by $P_{bal,t}$ using Equation (33):

$$P_{bal,t} = Q_{frac} *((1- P_{stdby,frac})*P_{nominal}) + P_{stdby,frac} * P_{nominal} \quad (33)$$

Determine the excess power defined by $P_{excess,bal,t}$ using Equation (34):

$$P_{excess,bal,t} = P_t - P_{bal,t} \quad (34)$$

The financial assumptions for the HTSE system are presented in Table 5 and Table 6. 2020 scenario costs are based on the INL model, and the 2050 scenario costs are based on the Hydrogen and Fuel Cell Technologies Office (HFTO) program record for 2050 (Peterson, Vickers, and DeSantis 2020).

Table 5. HTSE Capital and Installation Costs Based on the INL Study and HFTO Program Record

	Uninstalled Costs ($/kWDC)				Installation Factor	Indirect Costs (%)
Scenario	HTSE Stack	Electrical/Grid Connections	Water/Gas Feed and Heat Exchanger Systems	Purification and Compression		
2020	190	119	65	51	1.3	29.4
2050	100	257			1.3	29.4

Table 6. HTSE Operating Costs based on the INL Study and HFTO Program Record

Burdened Labor Cost	Overhead	Property Tax and Insurance	Material for Maintenance	Variable Operating Costs
$50/hour	20% of Labor	2% of Total Capital Cost	0.5% of Direct Capital Cost	0

The HTSE financial calculation is described in the following text. R_{DC_AC} is defined as the nominal DC stack capacity for a given nominal HTSE AC system capacity. The numbers used are based on INLs nth of a kind analysis (NOAK).

$$R_{DC\_AC} = 1012/1086$$

The overnight capital cost ($CAPEX_{overnight}$) is described by Equation (35) where $CAPEX_{uninstalled}$ is the uninstalled capital costs of the HTSE system, $i_{install}$ is the installation factor and $i_{indirect}$ is the indirect cost factor.

$$CAPEX_{overnight} = P_{nominal} * R_{DC\_AC} * CAPEX_{uninstalled} * i_{install} * i_{indirect} \quad (35)$$

The operating costs for a given year (y) over the analysis period (Y) are described by Equation (36) where $R_{planned,BOP}$ is the plannd replacement cost for the balance of plant and $R_{planned,stack}$ is the planned replacement cost for the stack**.**

$$OPEX = Labor + M\&R + PT\&I + R_{unplanned} + R_{planned,BOP} + R_{planned,stack} + O\&M_{variable} \quad (36)$$

where the labor costs are defined by Equation (37):

$$Labor = 2080\ hr/yr/FTE * 60\ (\$/hr) * 8\ (FTE) * (1+Overhead) \quad (37)$$

and maintenance and repair costs are defined by Equation (38):

$$M\&R = 0.005 * CAPEX_{overnight} / i_{indirect} \quad (38)$$

and property tax and insurance costs are defined by Equation (39):

$$PT\&I = 0.02 * CAPEX_{overnight} \quad (39)$$

and unplanned replacement costs are defined by Equation (40):

$$R_{unplanned} = 0.005 * CAPEX_{overnight} \quad (40)$$

and planned stack replacement costs are defined by Equation (41) and Equation (42):

$$R_{planned,stack} = \$155/kWDC * P_{nominal} * R_{DC\_AC} * i_{install}$$
$$\text{if } y \bmod 4 \; \forall \; y = 1..Y \text{ (Current Scenario)} \quad (41)$$

$$R_{planned,stack} = \$100/kWAC * P_{nominal} * R_{DC\_AC} * i_{install}$$
$$\text{if } y \bmod 7 \; \forall \; y = 1..Y \text{ (Future Scenario)} \quad (42)$$

and planned BOP replacement costs are defined by Equation (43) and Equation (44):

$$R_{planned,BOP} = i_{install} * (CAPEX_{uninstalled} - \$155/kWDC) * P_{nominal} * R_{DC\_AC}$$
$$\text{if } y \bmod 20 \; \forall \; y = 1..Y \text{ (Current Scenario)} \quad (43)$$

$$R_{planned,BOP} = i_{install} * (CAPEX_{uninstalled} - \$100/kWAC) * P_{nominal} * R_{DC\_AC}$$
$$\text{if } y \bmod 20 \; \forall \; y = 1..Y \text{ (Future Scenario)} \quad (44)$$

and variable O&M costs are defined by Equation (45):

$$O\&M_{variable} = 2.50 (\$/MWh\text{-}e) * P_{elec,y}/1000 \; \forall \; y = 1..Y \quad (45)$$

where $P_{elec,y}$ is the annual HTSE system electricity consumption (AC).

2.4 Solar Modeling in SAM

SAM is an open-source software developed by NREL that enables detailed technoeconomic analysis for renewable energy systems (Gilman et al. 2018). Project managers, policy analysts, technology developers and researchers use SAM technology simulation results when evaluating decisions regarding renewable energy systems. SAM has models for many types of renewable energy systems such as solar (photovoltaics, concentrating solar), geothermal, wind power and a basic generic model. SAM has several financial models for renewable energy projects such as power purchase agreements, residential projects and third-party ownership structures. In this analysis, SAM is used to simulate the solar energy production for a given location. JSON files for each solar energy model produced using the SAM desktop application are used to create PySAM solar unit modules in the PySAM framework. Alternatively, the solar unit modules are specified in PySAM directly without the use of a JSON file.

Three solar models in SAM were used this project: a PV-battery model; a molten salt hybrid model accounting for hybrid generation of electricity and heat; and a molten salt heat-only model. The PV-Battery model is selected for PV systems as it is the detailed version of the available PV models in SAM. PVWatts is an alternative option, but it makes several assumptions regarding the configuration and operation of the system. The PV-Battery model allows for detailed configuration of the PV field, inverter selection, and battery and cell level specifications and dispatch. The TcsmoltenSalt model is selected to represent both the molten salt hybrid model and molten salt heat-only model.

2.4.1 PV-Battery Model

The PV system model is based on the default PV-battery model in SAM (Gilman et al. 2018). A sizing function developed by running a SAM LK script calculates the number of modules per string, number of strings, and number of inverters for a single subarray given a nameplate DC capacity (kWDC) and target DC to AC ratio. The sizing functions are used as PV system parameters are not auto-enforced when nameplate capacities for PV model objects are updated in PySAM. The front-of-meter battery is AC connected and the dispatch is determined using hourly battery power targets. The battery power target at each hour is the difference between electrolyzer system's nominal AC power input and a perfect forecast of the PV generation in Year 1. SAM does not currently allow multiyear hourly dispatch time series; thus, the first-year dispatch is used for all 25 years of simulation. The financial assumptions for the PV and battery systems are presented in Table 7 and Table 8. The PV costs in the 2020 scenario and 2050 scenario are based on conservative 2020 and 2050 R&D scenarios from the 2021 Utility-Scale PV Annual Technology Baseline (ATB) ("2021 Annual Technology Baseline Utility-Scale PV" 2021). The 2020 scenario battery costs are based on 2021 Utility-Scale Battery Storage ATB ("2021 Annual Technology Baseline Utility Scale Battery Storage" 2021).

Table 7. PV System Cost Assumptions

Scenario	MWe Nameplate	Hours Storage	Tracking	DC to AC	Total Installed Cost ($/kWAC)	Variable Cost ($/MWh)	Capacity Fixed Cost ($/kw-yr)
2020	Variable	Variable	1 Axis	1.34	1,377	0	23
2050	Variable	Variable	1 Axis	1.34	776	0	17

Table 8. Battery System Cost Assumptions

Scenario	Power (kWDC)	Capacity (kWhDC)	Power Cost ($/kWDC)	Capacity Cost ($/kWhDC)	Replacement Cost ($/kWhDC)
2020	Variable	Variable	257	277	277
2050	Variable	Variable	26[a]	28	28

[a] Based on DOE Earthshot, Storage battery cost reduction targets ("Long Duration Storage Shot: An Introduction" 2021)

2.4.2 Molten Salt Hybrid Model

For the molten salt hybrid model, the molten salt power tower model outputs are post-processed to account for the hybrid generation of electricity and heat. The default molten salt tower unit module in PySAM is used as the building block for the hybrid model (Turchi and Heath 2013). The heat transfer fluid (HTF) is split by a stream splitter into two streams before the power block. The first stream goes through the power block to generate electricity, while the second stream goes to a heat exchanger to vaporize feedwater. The split ratio is assumed to be constant based on the needs of the HTSE at nominal load. The return temperature of the HTF is also assumed to be constant. This approach therefore generally consists of "virtually oversizing" the SAM salt tower power block to account for the additional heat load to the HTSE through the HTF. The performance and financial assumptions for the molten salt hybrid model are presented in Table 9. The molten salt tower costs are based off the conservative 2020 and moderate 2050 scenarios in the Concentrating Solar Power 2021 ATB ("2021 Annual Technology Baseline Concentrating Solar Power" 2021).

Table 9. Hybrid Molten Salt Tower Assumptions

Scenario	Power Cycle Design Efficiency	HTF	Hours Storage	Total Installed Cost ($/kw)	Variable Cost ($/MWh)	Capacity Fixed Cost ($/kw-yr)	Loop Outlet HTF Temperature
Current (2020)	0.412	Salt (60% $NaNO_3$, 40% KNO_3)	Variable (8–12 hours)	6,573	3.5	66	574°C
Future (2050)	0.412	Salt (60% $NaNO_3$, 40% KNO_3)	Variable (8–12 hours)	4,213	2.9	50	574°C

HTF = Heat Transfer Fluid

2.4.3 Molten Salt Heat-Only Model

The molten salt heat-only model uses the molten salt power tower model to estimate the operation of a heat-only salt tower. The power block is turned off, and parisitics/costs associated with the power block are removed. The turbine output is used to specify a heat flow rate based on the cycle thermal efficiency. The return temperature is assumed to be constant.

Since the default tower parameters in SAM aren't accurate for towers modeled under 10 MWth with surround receivers, several adjustments are made to the default SAM model. Initially, some issues were encountered with sizing the smaller salt towers in SAM because of spillage and the solver startup energy requirements. To address those issues, the following steps were taken:

- The tube outer diameter is selected to ensure that the Reynolds number was safely above the transition zone based on the minimum receiver mass flow rate and fluid properties at the design inlet temperature. The Reynolds number is roughly 50000.
- Linear interpolation is used to estimate the number of receiver panels, number of heliostat facets, heliostat width/height, receive diameter/height, and startup/tracking powers between the 1 MWth, 4 MWth, and 10 MWth cases.

Finally, a cost equation that is more representative of smaller towers, rather than the cost equation used for larger towers shown below, is used (Sargent & Lundy 2003). The last term in the equation represents the cost index adjustment using the chemical engineering index.

2020$ = (600000 + 17.72 * (height_meters^2.392)) * (596.2/355)

2.5 Solar to Hydrogen Systems Selection

Four solar hydrogen systems are analyzed in this project using combinations of the electrolyzer and solar models described in the previous sections. The four systems are detailed in Table 10.

Table 10. The Four Hydrogen Production Systems Modeled using the H_2 in SAM Framework

System	Description
Grid-LTE	An LTE module connected to the grid that operates in response to grid electricity prices in a price-taker scenario.
PV-LTE With Optional Battery Storage	A PV farm coupled to an LTE module through an AC-DC connection with optional AC-connected battery storage ranging from 1 to 12 hours. The overall system is islanded with a small grid connection for parasitics.
MSALT-HTSE	A hybrid molten salt tower coupled to an HTSE module wherein the hybrid molten salt tower provides heat and electricity to the HTSE module. An auxiliary boiler and grid connection are used to handle HTSE hot standby and tower parasitics. The overall system is assumed to be islanded.
PV-MSALT-HTSE	A PV farm and heat-only molten salt tower coupled to an HTSE module wherein the PV farm provides electricity and the tower provides heat to the HTSE module. An auxiliary boiler and grid connection are used to handle HTSE hot standby and tower parasitics. The overall system is assumed to be islanded.

The Grid-LTE system represents the standard low-temperature electrolysis system deployed today. In our analysis, the LTE module will be operated to minimize the overall hydrogen levelized cost each year versus running the electrolyzer at a fixed capacity factor or constant load. This system can serve as a baseline to compare the three solar hydrogen systems.

The PV-LTE system represents the highest TRL solar hydrogen system of the three and is already seeing deployment worldwide. This configuration is common for solar-hydrogen systems because of the modularity of both the PV and LTE subcomponents. Battery storage based on lithium-ion nickel-manganese-cobalt (NMC) batteries is optional for the system. The storage utilizes trimmed PV electricity during nighttime hours rather than load flattening or balancing, PV-LTE is the baseline LTE-

based solar hydrogen system. To understand the implications of connecting concentrating solar power to an electrolyzer system, which is currently low- to mid-TRL, the MSALT-HTSE system was formulated. Conversely, PV-MSALT-HTSE was designed to understand whether coupling low-cost PV electricity, as well as using a tower for an HTSE rather than a hybrid tower, would be more economical.

2.5.1 System Simulations

The calculation flow diagram for the Grid-LTE system is presented in Figure 6. The electrolyzer system size selected impacts the overall capital and operating costs based on a scaling factor. An LTE operating schedule is determined by selecting the number of operating hours and an hourly locational marginal price curve obtained using historical data obtained from wholesale electricity operator APIs. The electrolyzer is assumed to operate at the lowest electricity prices for the given number of operating hours in a year. Once the operating schedule is determined, the electrolyzer is assumed to draw nominal power at the operating hours, and a capacity charge at each hour is calculated using the electricity price at each hour. The AC power is rectified using a rectifier efficiency curve, and the DC power is split evenly between each stack, which is assumed to be identical and operating under identical conditions. Given a constant temperature at each hour for each stack, the hourly hydrogen generation is calculated using the power input and temperature with either the H2A or performance curve-based LTE model. The capital and annualized costs for the system are assigned to the appropriate parameters of the generic single-owner SAM module. The generic module is run to determine the hydrogen levelized cost. The generic single-owner SAM module is a levelized cost calculator that can be used to represent any system. Although the primary output is the HLC, any SAM model output or parameter and electrolyzer model output or parameter is amalgamated into a dictionary as an optional output.

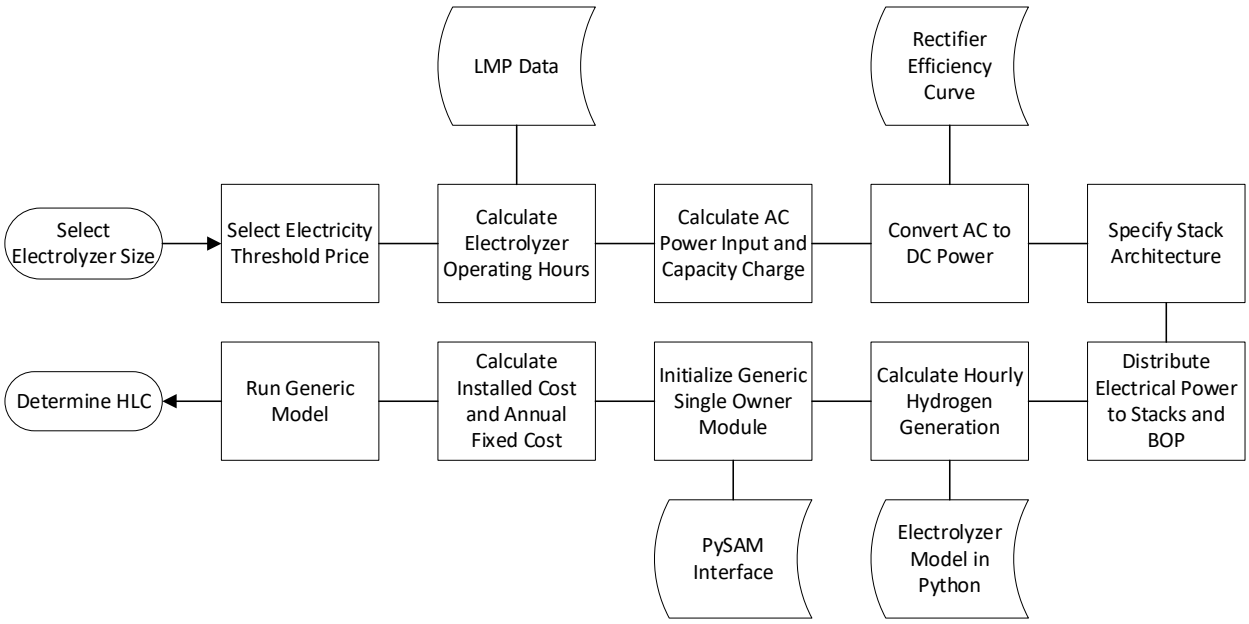

Figure 6. Grid-LTE system calculation flow diagram

The calculation flow diagram for PV-LTE is presented in Figure 7. A PV system size and resource file are used to initialize the PV SAM model. The PV system CAPEX and OPEX costs are determined using the latest Annual Technology Baseline (ATB) projections. The AC power from the PV system is rectified and sent to a peak-sized or user-selected electrolyzer stack size.

A calculation flow similar to the Grid-LTE system is used to determine the hourly hydrogen production and hydrogen levelized cost. The main limitation is that the levelized cost calculations in the generic SAM model only accept 1 year of hydrogen production values. Because of PV module degradation, the hourly hydrogen production rate decreases as a constant rate over the system lifetime of 25 years. To account for this behavior, the average hydrogen production rate across 25 years is used as an input into the levelized cost calculator. This limitation does not apply to LTE model degradation as the stack is oversized to account for degradation in the H2A model. In addition, the LTE system or stack is replaced at specified schedules to ensure nominal performance in accordance with H2A assumptions. The financial coordination module combines the costs of the two systems and assigns them to the generic model while adjusting generic module parameters to account for differences between the subcomponents, such as depreciation schedules. The solar hydrogen system is assumed to be purchased as one system (i.e., the subcomponents have the same financing structure and rates). If battery storage is included, the battery is dispatched using the LTE nominal capacity and a perfect PV forecast for the year. Because the battery dispatch can only be single-year in SAM, the first year battery dispatch is used for all 25 years of battery storage.

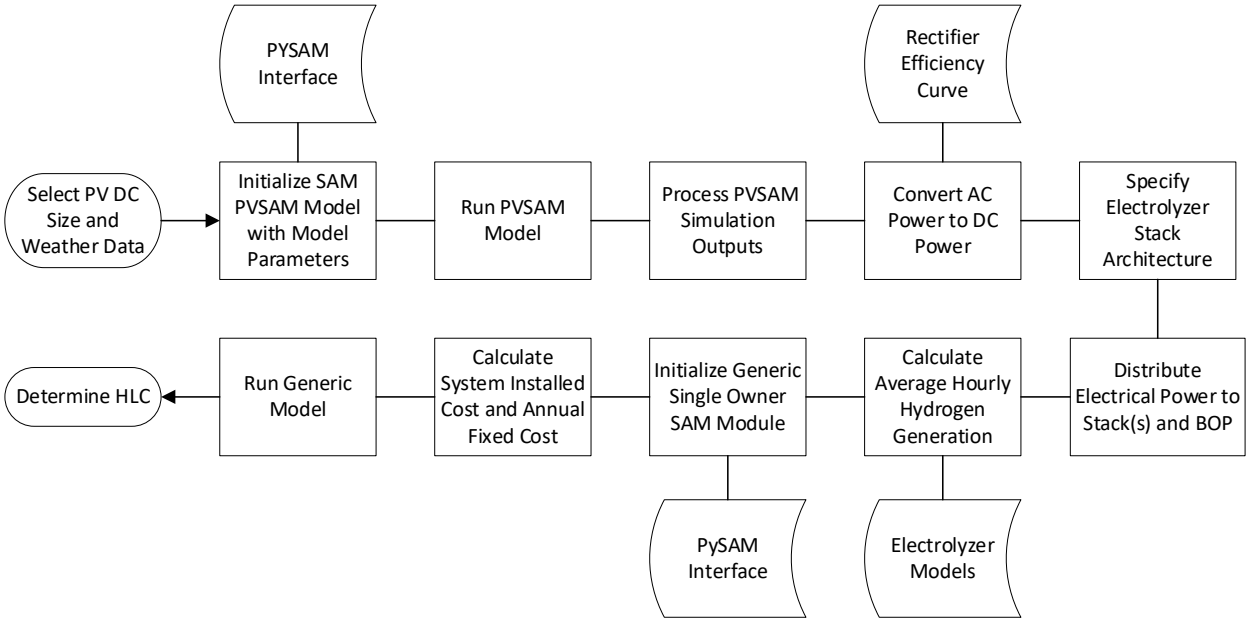

Figure 7. PV-LTE system calculation flow diagram

The calculation flow diagram for MSALT-HTSE is presented in Figure 8.The tower's nominal electrical and heat capacity are selected along with a resource file to initialize the SAM tower power model. The tower power parameters are adjusted (e.g., dispatch schedule, costs, field) and the power tower model is run. In this report, the tower is dispatched to a constant hourly load when possible as HTSE systems operate more efficiently at a constant load. The outputs of the model are post-processed to account for hybrid generation. This post-processing approach is used because a power tower model that produces both process heat and electrical power is not available in SAM for use with the HTSE, and creating one would be a significant effort. Instead, the Power Tower Molten Salt model in SAM is employed. Although this model is power-only, the results are post-processed in a way to emulate a heat and power plant. The emulation is done by oversizing the power cycle by an amount corresponding to the process heat needed from the plant, scaled by the design power cycle efficiency. This modification is the only one needed to set up the heat and power tower model.

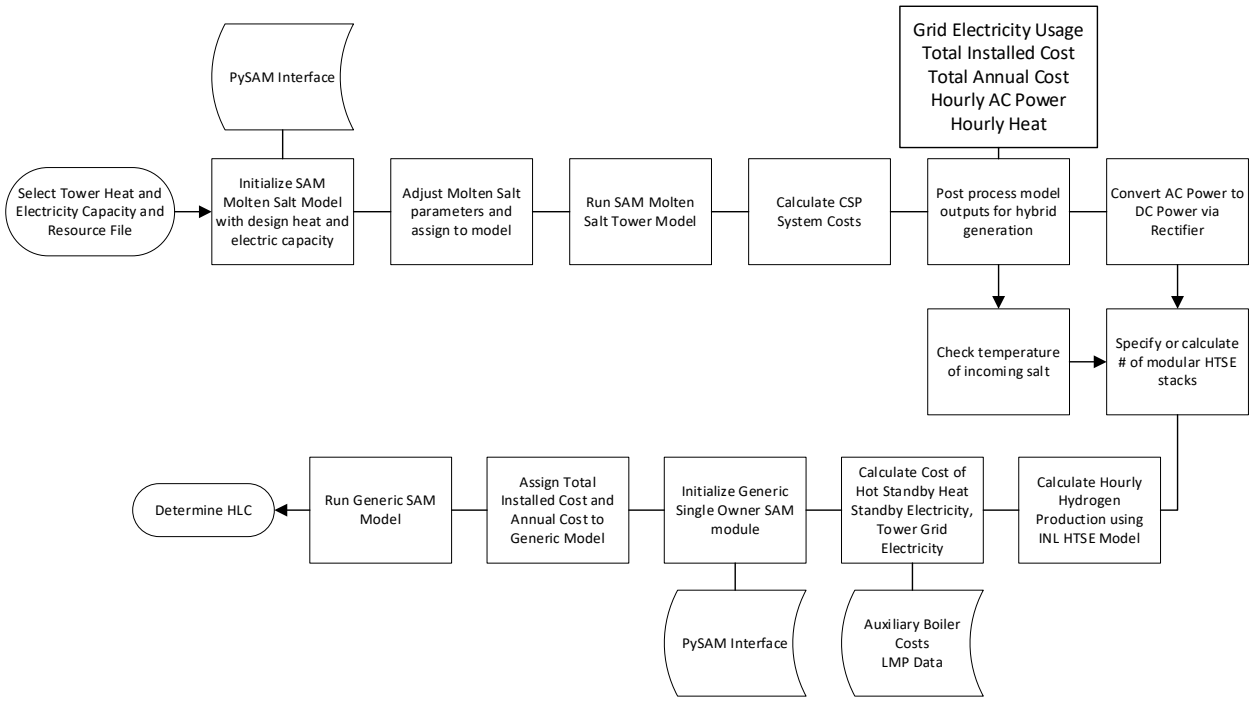

Figure 8. MSALT-HTSE system calculation flow diagram

During simulation, the tower plant controls the oversized (SAM-modeled) power cycle the same way it does for the smaller (emulated) power cycle, including startup time. After an annual simulation is complete, the results are post-processed to simulate the heat and power tower plant. The electrical power output is reduced according to the heat-to-power ratio needed by the HTSE and the cycle efficiency at the time. This reduction effectively back-calculates the amount of salt HTF that would have entered the cycle heat exchanger but instead now enters a second heat exchanger that is used for the HTSE steam input. In addition, power cycle startup heat requirements, condenser water usage, and various cycle parasitics and costs are reduced accordingly for a smaller emulated cycle.

Note that the molten salt stream into the cycle salt-steam heat exchanger is split to generate the process steam instead of splitting the required steam off the power cycle. Splitting steam from the high-pressure turbine outlet could be more economical, but that approach would involve considerable modeling effort and was outside the scope of this project because of the power cycle being a reduced-order model without exposed steam flows. Splitting the hot inlet salt stream in post-processing, however, requires the two cold outlet salt streams to recombine at the same temperature for actual/emulated model continuity, and this recombination is assumed to occur in the HTSE process model.

The AC power is rectified and the heat is used to vaporize feedwater for the HTSE. The HTSE system is initialized at this point and uses the SAM model outputs to calculate the hourly hydrogen production. Other hourly outputs, such as the HTSE hot standby heat and electricity requirements, the cost of addressing unmet hot standby energy requirements, and tower parasitics, are also calculated. The HTSE and tower costs are coordinated in the financial coordination module in a similar manner to PV-LTE. The generic single-owner module is also used to calculate the hydrogen levelized cost. The tower is assumed to experience negligible performance degradation, and the HTSE stack and system are replaced at specified intervals to ensure nominal performance.

The calculation flow diagram for PV-MSALT-HTSE is presented in Figure 9. A heat-only tower heat capacity and a PV capacity are simultaneously selected, along with a resource file to initialize both the PV and tower models. For the heat-only tower, the size-dependent parameters, such as the tube outer diameter, are adjusted and the power block is removed. The PV SAM model is then run, and power output is used to calculate the dispatch for the heat tower. The dispatched heat and PV power are sent to the HTSE model, which calculates the hourly hydrogen production. The rest of the calculation flow is similar to the MSALT-HTSE system.

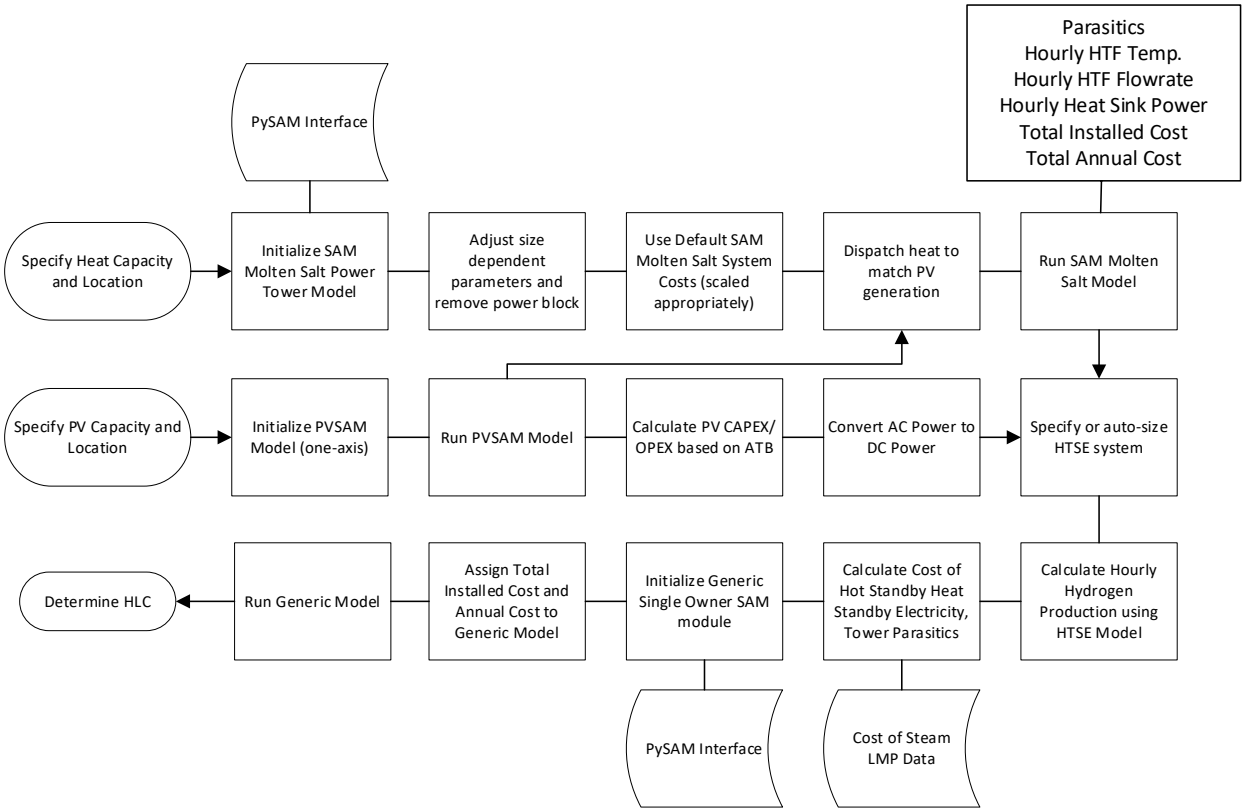

Figure 9. PV-MSALT-HTSE system calculation flow diagram

2.5.2 System Sizes

The baseline sizes for each system are presented in Table 11. The baseline sizes are generally selected to match the system-size assumptions for the cost models that are used, such as H2A and ATB. The baseline Grid-LTE capacity factor and LTE system size are chosen to match H2A central production models. The PV nominal capacity in PV-LTE is selected to match the baseline utility one-axis PV case in the ATB. The nominal electric capacity and hours of storage of the hybrid salt tower in MSALT-HTSE are based on SAM system defaults. Lastly, the PV size in PV-MSALT-HTSE is also based on the ATB baseline for utility PV systems. The grid search specification implies that the subcomponent size will be selected based on a grid search that seeks to optimize the HLC.

Table 11. Baseline System Component Sizes

System	Electric Capacity (Solar)	Thermal Capacity (Solar)	System Size	Battery Capacity	Thermal Storage	Battery Power
Grid-LTE	Optimized based on operating hours	N/A	131 MW	N/A	N/A	N/A
PV-LTE-Batteries	100 MWDC	N/A	Grid Search	Variable	N/A	Variable
MSALT-HTSE	115 MWe	Grid Search	Grid Search	N/A	10 Full Load Hours	N/A
PV-MSALT-HTSE*	100 MWDC	Grid Search	Grid Search	Variable	10 Full Load Hours	Variable

2.6 General Financial Parameters

Regarding cost models, several levelized options are available to use, such as the generic single-owner SAM model, H2A, and H2FAST. A comparison of the SAM and H2A levelized cost models is provided in the following text to identify differences in HLC values for identical systems, HLC sensitivities, and differences in assumptions. Table 12 shows the parameters used in both the SAM and H2A levelized cost calculations.

Table 12. Parameters Used in SAM and H2A for HLC Calculations for All Systems

Parameter	SAM and H2A
Analysis Period/Plant Life	40
Real Discount Rate	8%
Inflation Rate	1.9%
% Equity	40%
Debt Interest	3.7%
Debt Tenor/Type	40 Years/Constant
Effective Tax Rate	25.74%
Depreciation Schedule	20-Year MACRS
Salvage Value	10%
Dollar Year	2020$

MACRS = Modified Accelerated Cost Recovery System

To assign H2A parameters to SAM's generic, single-owner model, levelized cost calculation, several steps were performed:

1. H2A's annual hydrogen production was converted to an hourly value for SAM input.
2. The non-variable annualized costs in H2A were amalgamated into a vector of yearly annual costs and input into SAM's fixed annual cost parameter.
3. All variable costs in H2A were summed and normalized to H_2 production for input.
4. A custom 20-year MACRS depreciation schedule was specified for SAM.
5. Construction financing was removed from SAM.
6. The SAM parameter values in Table 12 were adjusted to the values used in H2A.
7. The hydrogen generation in Year 1 in SAM was manually adjusted to 50% by adjusting the total hydrogen produced in the levelized cost calculation.

A key difference that cannot be adjusted in SAM to match H2A is the working reserve. The working capital reserve in SAM is 6 months of operating costs (the number of months is adjustable), and interest is earned on the reserve. In H2A, the reserve is 15% of the difference in operating costs between each year.

The major difference between the two levelized cost calculations, which needs to be addressed, is that the denominator of the levelized cost equation has a tax applied to it in H2A but not in SAM. The denominator is the total amount of hydrogen produced across the analysis period. One way of interpreting this difference is that the value of hydrogen produced in H2A is reduced by the tax rate, while this reduction is not made in SAM. The results in this report assume that hydrogen revenue is not reduced by the tax rate which is in line with the generic single owner model assumptions in SAM.

2.6.1 Baseline Analysis Location: Daggett, California

Daggett, California, was used as the solar hydrogen system location for the baseline analysis performed in this report. Daggett has excellent solar resources, which is a key factor in whether a solar hydrogen system would be economical to build. The analysis of the four solar-hydrogen systems was also performed for 40 locations to identify potential spatial variations of HLCs for each system. These locations were selected based on proximity to hydrogen infrastructure (e.g., salt caverns, pipelines); covering the solar resource spectrum of the continental United States; geographical coverage (range of latitude and longitudes); and industrial hydrogen demand locations (e.g., the locations in southern Texas are near hydrogen pipelines).

Locations with geological hydrogen storage were identified based on a scoping report conducted by Sandia National Laboratories (Kobos et al. 2011). The serviceable consumption potential for the industrial sector from the H2@Scale report (Ruth et al. 2019) was used to select areas in proximity to counties with hydrogen demand. Because the analysis in H2@Scale was performed at a county level, the demand was assumed to be distributed evenly across each county for the single location selection. A map of hydrogen and interstate natural gas pipelines, which was developed by NREL GIS, was used to identify locations in proximity to pipeline infrastructure. Finally, additional locations were selected to cover the solar resource and geographical variability in the continental United States.

2.6.2 Grid-LTE System Analysis: SAM and H2A

A Grid-LTE system using the electricity locational marginal price curve in Daggett 2019 (OASIS 2022) COLWATER_001_N02 node with a 97% capacity factor was analyzed in both SAM and H2A. The HLC results for the two tools are shown in Table 13. The HLC_no_adjustments row in the SAM column represents the HLC calculated using default SAM parameters. The HLC_tax_adjusted row represents the HLC cost after the difference in the tax approach on the HLC denominator is adjusted in SAM. Lastly, the HLC row represents the HLC after all differences between SAM and H2A are adjusted for in the SAM model. Once all adjustments are made, the HLC agrees between SAM and H2A.

Table 13. Hydrogen Levelized Cost Values in SAM and H2A

Parameter	SAM	H2A
NPV_no_adjustments (after-tax)	374,229,248	354,364,041
HLC_no_adjustments	1.57	N/A
HLC_tax_adjusted	2.13	N/A
HLC	2.20	2.16

NPV = Net Present Value

To further evaluate the differences between the two levelized cost calculations, key parameters of HLCs, such as equity, discount rate, installed cost of the LTE stack, and variable O&M are varied as shown in Table 14. The study is done to identify how the adjusted SAM HLC changes relative to the changes in the H2A HLC.

Table 14. Sensitivity Analysis Parameter Lower and Upper Bounds for SAM and H2A HLC Comparison

Parameter	Default	Lower	Upper
Equity	40%	20%	80%
Discount Rate	8%	6%	10%
Total Installed Cost	$600/kW	$100/kW	$900/kW
Variable O&M	1x	0.5x	1.5x

The result of this sensitivity analysis is shown in Figure 10. A maximum percent difference of 3.5% between H2A and SAM is obtained when varying key HLC parameters; thus, the methodology to adjust seems to be sufficient in producing SAM HLCs that agree with H2A HLCs.

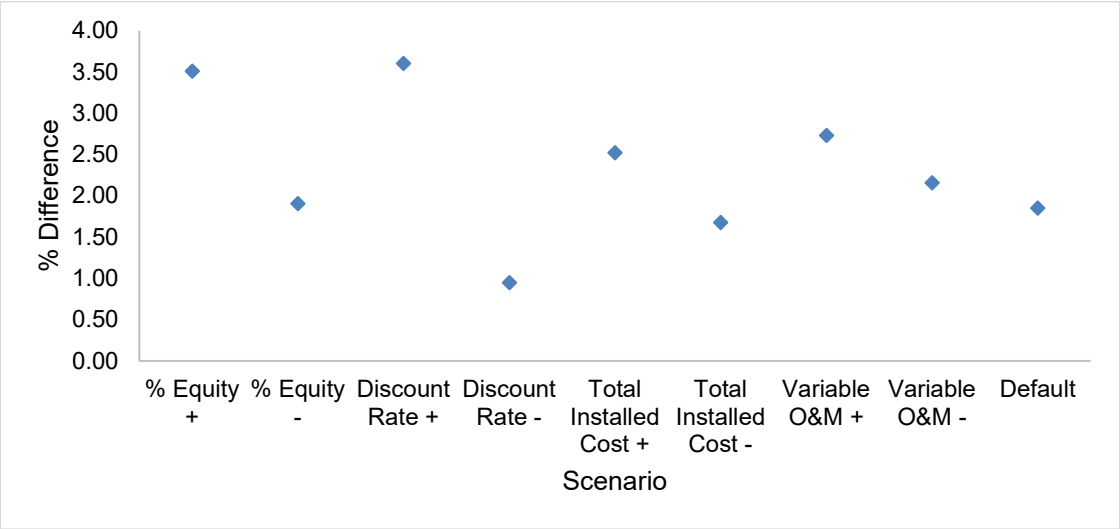

Figure 10. Percentage difference between H2A and SAM levelized cost calculations when varying key HLC parameters

3 Results and Discussions

The study results discussed in this chapter focus on when each of the systems included in this analysis can be cost-competitive with conventional hydrogen production pathways by setting a cost target of \$2/kg H_2. Both current and future scenario hydrogen levelized costs and hydrogen levelized cost sensitivities are discussed for each system. The systems are simulated across 40 locations on the continental U.S. to identify lowest cost systems in the current and future scenario with pathways to \$2/kg H_2.

3.1 System 1: Grid-LTE

A block flow diagram of the Grid-LTE system is presented in Figure 11. The LTE is operated to minimize the HLC by utilizing lower-cost electricity while maintaining enough operating hours to cover the capital cost of the system. The location that was selected for this set of results is Daggett, California, because of its previously mentioned excellent solar resources.

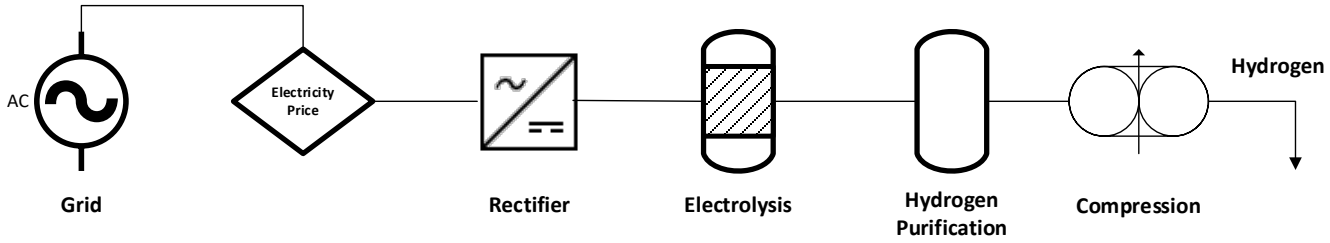

Figure 11. Grid-LTE block flow diagram

The electricity price curve used for Daggett, California, is the COLWATER_1_N002 LMP curve from 2019. A plot of the electricity prices at this node, ordered from the highest electricity prices to the lowest prices, is shown in Figure 12 in the top image. A heat map of the hourly electricity prices is presented in Figure 12 in the bottom image. The hourly electricity prices have some extremes, as represented by the tail ends of the curve. From the heat map, the higher electricity prices tend to occur in late evening hours and during the winter months. The lower electricity prices tend to occur during the early summer months. The bulk of the hourly prices, however, are approximately \$40/MWh, as represented by the flat section of the curve. Because of the variability in the electricity prices, a specific operating schedule will minimize the HLC for the Grid-LTE system.

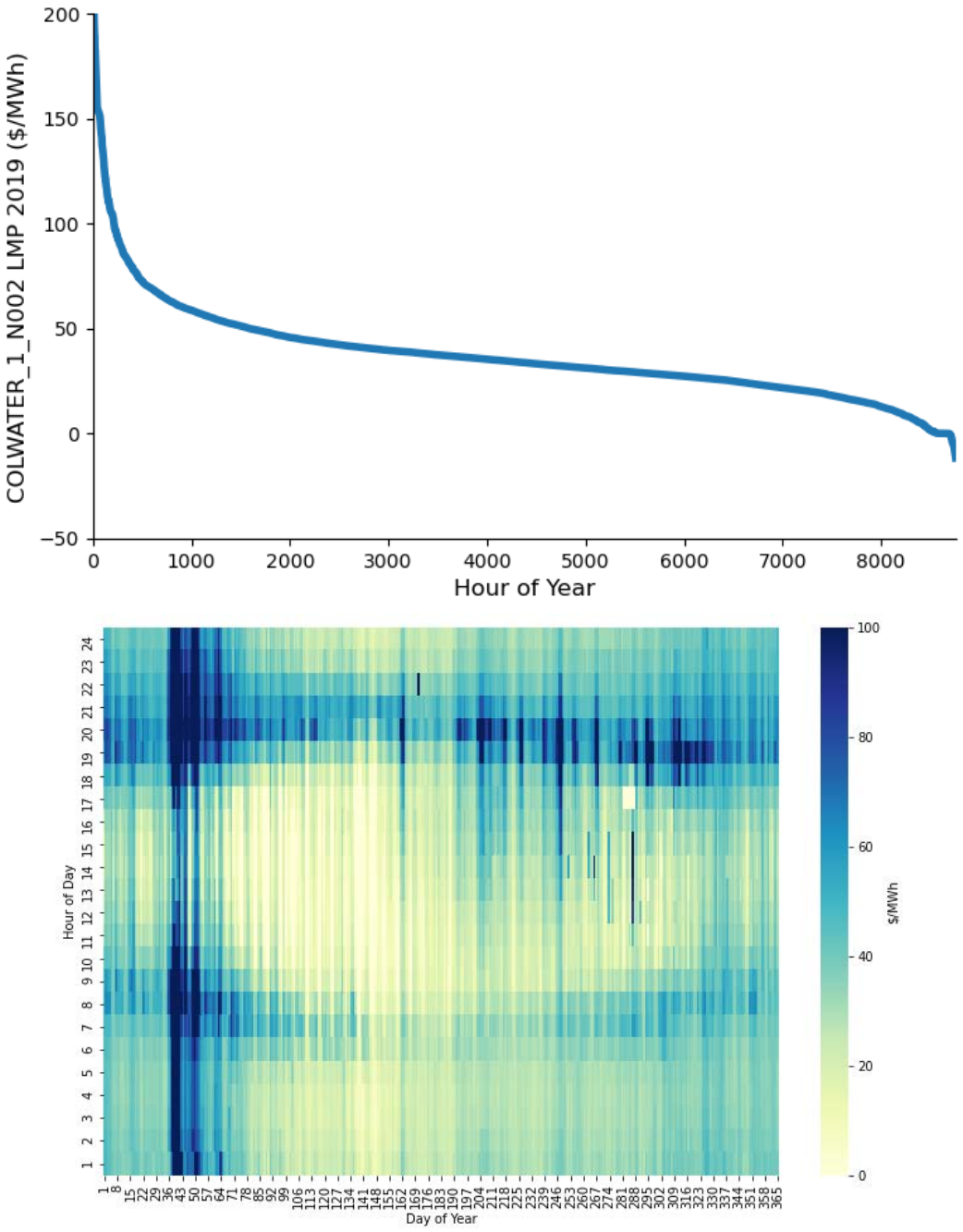

Figure 12. Locational marginal price curve ordered from most expensive hour to least (top figure) and visualized using a heat map (bottom figure)

The HLC at every operating hour between 1 hour and 8,760 hours of operation per year is computed at electrolyzer stack purchase costs of $143–$782/kW. The resultant curves depicted in Figure 13 provide insight into the impact of the electrolyzer capacity factor on the HLC. At a few operating hours per year, the electrolyzer operates using negative or near zero-priced electricity. However, the HLC increases when approaching fewer operating hours, as the high capital cost is spread across a small amount of hydrogen product. If the electrolyzer operates for all hours of the year, the capital cost is spread across a large amount of hydrogen product. But high electricity prices are used to produce hydrogen resulting in

high HLCs. The optimal HLC exists in between the two extremes described above and tends to shift toward higher operating hours with increasing electrolyzer purchase costs. In this scenario, the minimum price is represented by the optimal HLCs depicted in Figure 13, which can be considered a baseline value for comparing the economic performance of solar-hydrogen systems. The optimal HLCs are \$3.40, 2.82 and 2.50/kg H_2 for stack purchase costs of \$782, 342 and 143/kW respectively. These optimal HLCs do not factor in the cost impacts of cycling such as increased cell degradation which would shift the optimum number of operating hours higher to reduce the number of cycles.

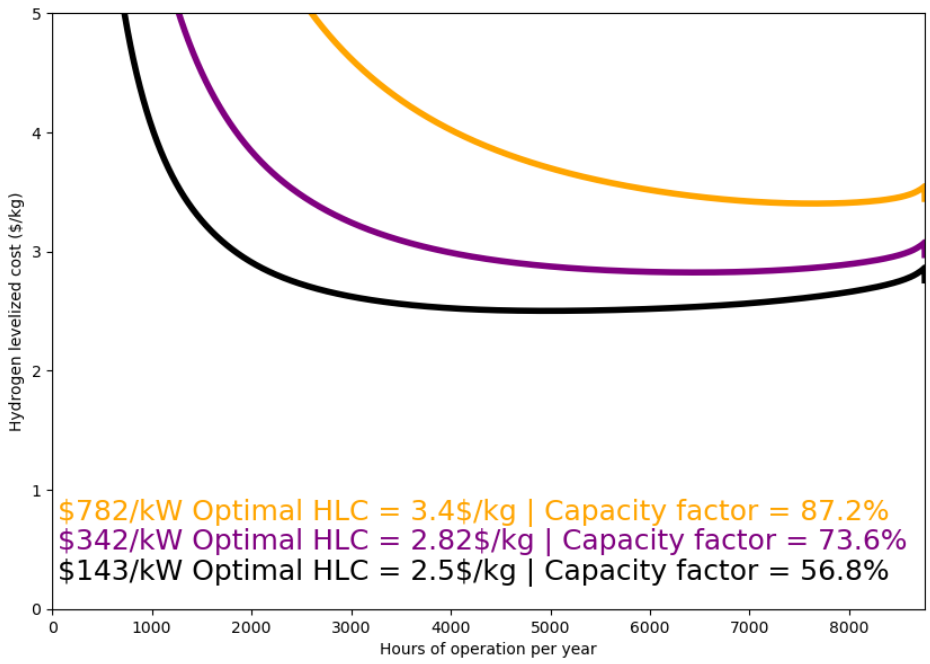

Figure 13. HLC curves for varying stack purchase costs for the Grid-LTE system at Daggett

3.2 System 2: PV-LTE

A block flow diagram of the PV-LTE system is presented in Figure 14. The PV-LTE system is the only solar to LTE system explored in this report. In this setup, a PV with an inverter is coupled to an electrolyzer via a rectifier. AC battery storage is used and is currently dispatched to charge-trimmed PV electricity to discharge when the electrolyzer is under nominal capacity.

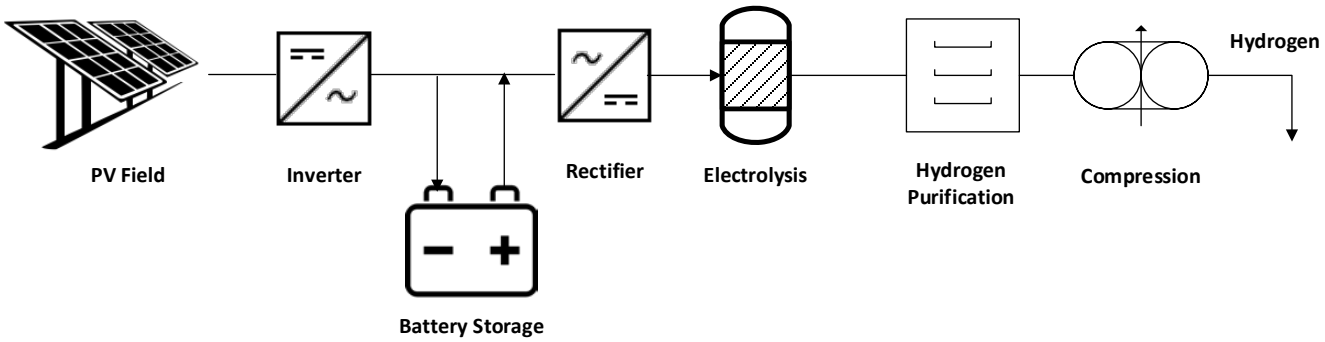

Figure 14. PV-LTE system block flow diagram

The baseline case explored is a 100-MW PV system coupled to an electrolyzer without a battery in Daggett, California, in 2020. The optimal size of the electrolyzer is highly dependent on the cost of the electrolyzer and available PV energy at the location. The following discussion is based on the PV-LTE system without a battery.

Figure 15 shows the variation in the HLC as the electrolyzer capacity is changed from 45,000 to 65,000 kW in the baseline case. Hypothetically, the electrolyzer can be sized to peak PV production during the summer months; however, at this size, the high electrolyzer capital cost may not be sufficiently spread over the hydrogen product, which results in higher HLCs. Conversely, an electrolyzer that is sized to winter PV generation results in high HLCs because the PV capital cost is not sufficiently spread over hydrogen product. The simple sizing exercise shown in Figure 15 indicates that in the baseline case, an electrolyzer that is between 50 MW and 60 MW is ideal for a 100-MW PV array with electrolyzer capital costs of $342/kW and PV capital costs of $1.377/WAC. The HLC at an electrolyzer capacity of 55 MW is $3.86/kg H_2 and is the baseline HLC for the 2020 case. As the electrolyzer purchase cost decreases, the optimal electrolyzer capacity factor shifts higher as the capital cost of electrolyzer capacity is lower. In locations with fewer solar resources than Daggett, the optimal electrolyzer capacity decreases as less electricity is being produced by the PV plant.

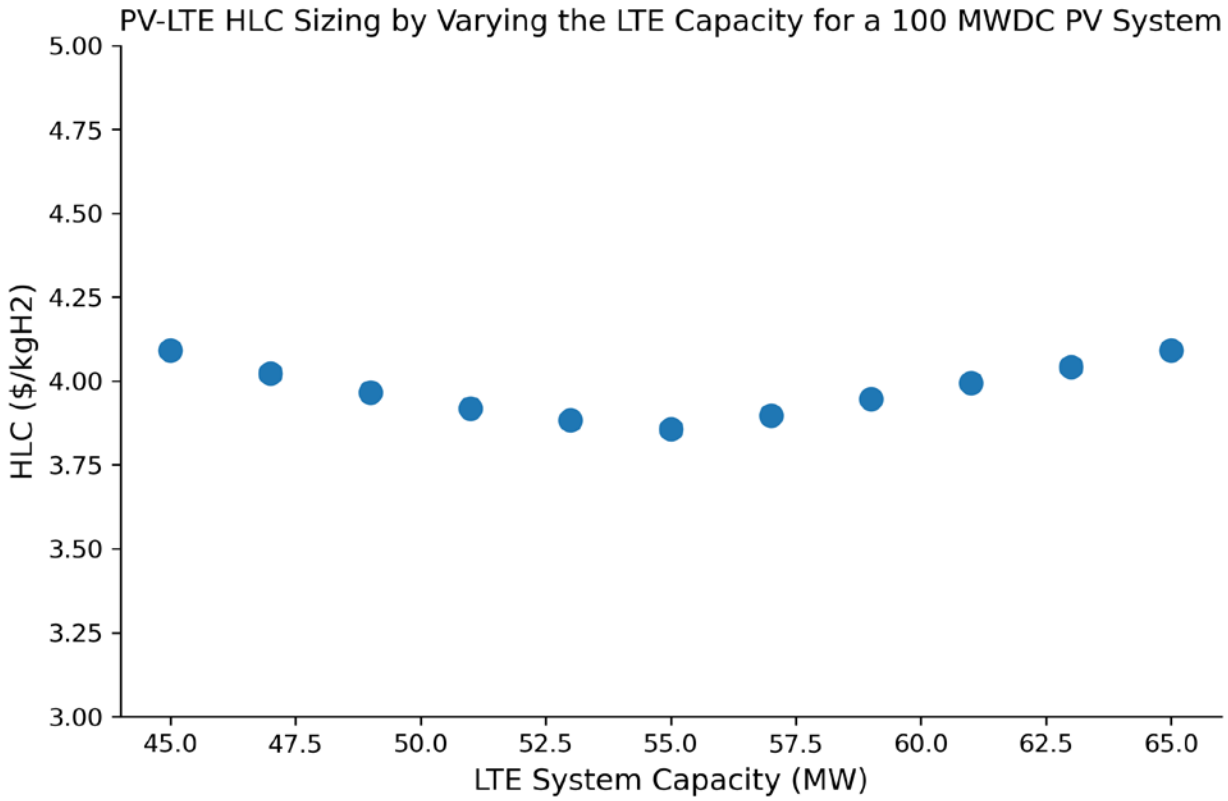

Figure 15. PV-LTE system-sizing curve for a PV capital cost of $1.377/WAC and an LTE stack purchase cost of $342/kW.

The performance of the PV-LTE system is explored at the optimal PV:LTE ratio of 100 MWDC to 55 MW. At this PV:LTE size ratio, 0.2% of the electricity is trimmed with increasing amounts of trimmed electricity as the electrolyzer capacity decreases. This result is observed when the analysis location for the PV-LTE systems is varied as well. In general, we observe that the cost-optimal PV:LTE ratio occurs when negligible electricity is trimmed for an islanded system. If electricity can be exported, the optimum PV:LTE ratio would likely change. In other words, the optimal LTE capacity for a given PV installation leans towards sizing the LTE towards peak generation in the summer months.

At this PV:LTE ratio, the electrolyzer operates at a capacity factor of 38.5%. Hydrogen is produced exclusively when PV energy is available, as battery storage is not included in this configuration. The result is hydrogen production from 6:00 a.m. to 8:00 p.m. during the summer months and 8:00 a.m. to 6:00 p.m. during the winter months as can be seen in Figure 16. The hydrogen production remains relatively constant in the summer months during daylight hours and tapers off during early morning and nighttime hours. In the winter months the hydrogen production is also consistent, but at a reduced capacity compared to the summer months. The variability and limited hours of hydrogen production restrict the capability of coupling PV-LTE systems to industrial plants that operate at 20- to 24-hour constant loads in the absence of storage. Industrial activities that require hydrogen, such as metal and oil refining, typically operate at a constant load with a high capacity factor. The addition of high power and capacity batteries to extend the hours of hydrogen production will be explored in this section to address this issue.

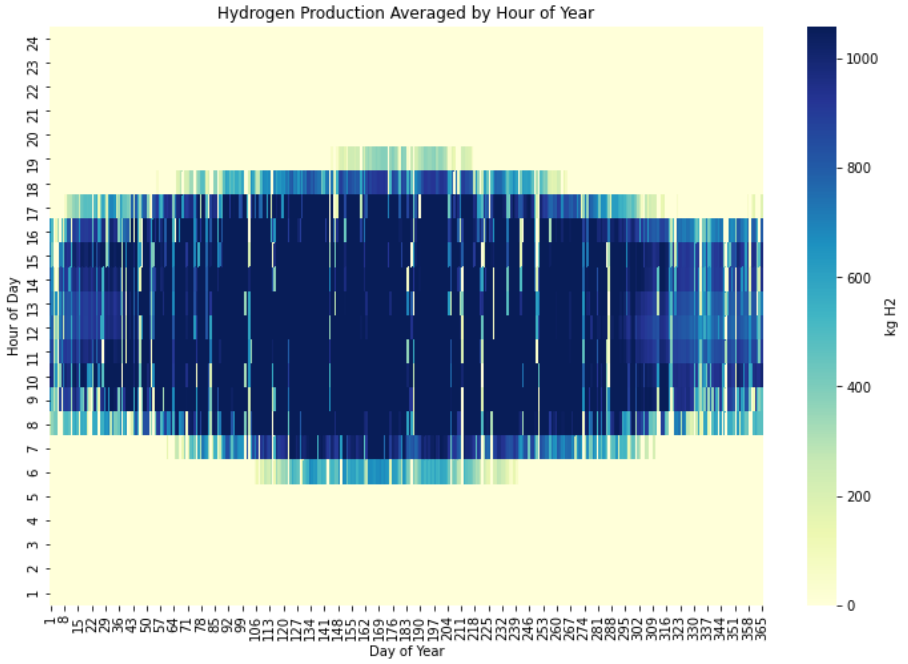

Figure 16. Annual hydrogen production in the first year for the baseline PV-LTE system in Daggett

The overall annual hydrogen production is approximately 3600 tonnes/yr and decreases over time due to PV degradation as shown in Figure 17 below. This is equivalent to the production rate of a 20 MW grid electrolysis system operated at a 97% capacity factor.

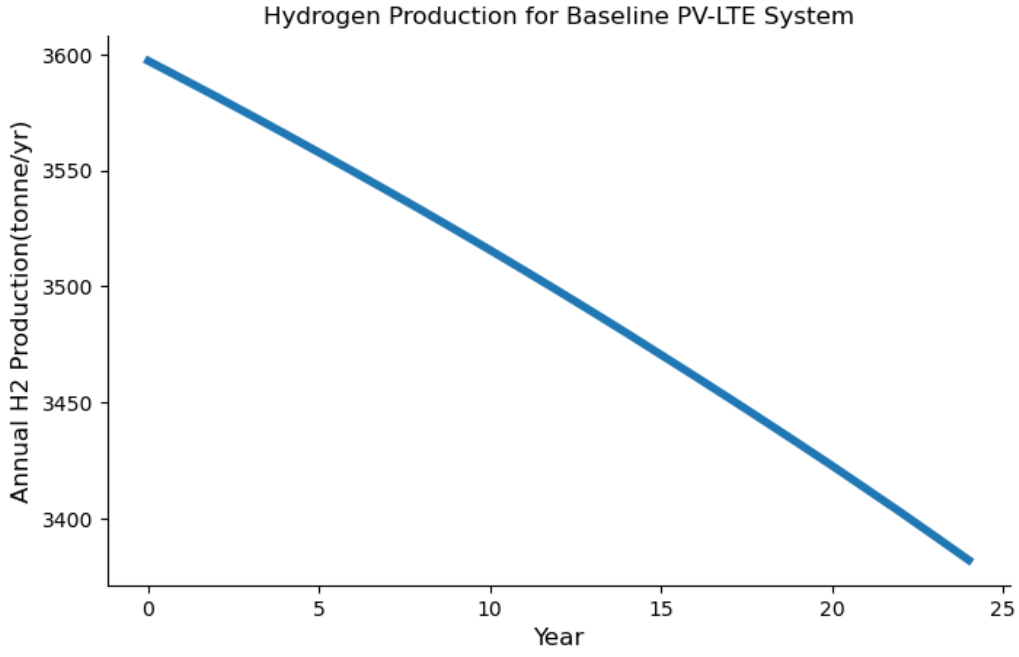

Figure 17: Annual hydrogen production for the baseline PV-LTE system

As identified in the Grid-LTE system, the optimal HLC for different electrolyzer purchase costs ranges from \$2.50 to \$3.40/kg H_2, depending on the stack purchase costs. Steam methane reforming, or the conventional method of hydrogen production, can typically produce hydrogen at under \$2/kg H_2. The

current 2020 baseline value of $3.86/kg H_2 is significantly above the target HLCs that would enable a hydrogen economy.

Tornado and contour plots were developed to identify the parameter space where the HLC of PV-LTE systems can approach $2/kg H_2. Figure 18 highlights the key costs that influence the economics of the PV-LTE system. Key parameters that could influence the HLC of the system vary between 2050 and 2020 values. The capital costs of the LTE and PV systems are the key cost drivers for the HLC of the PV-LTE system. Neither LTE nor PV capital cost reductions alone can drive the HLC to below $2/kg H_2.

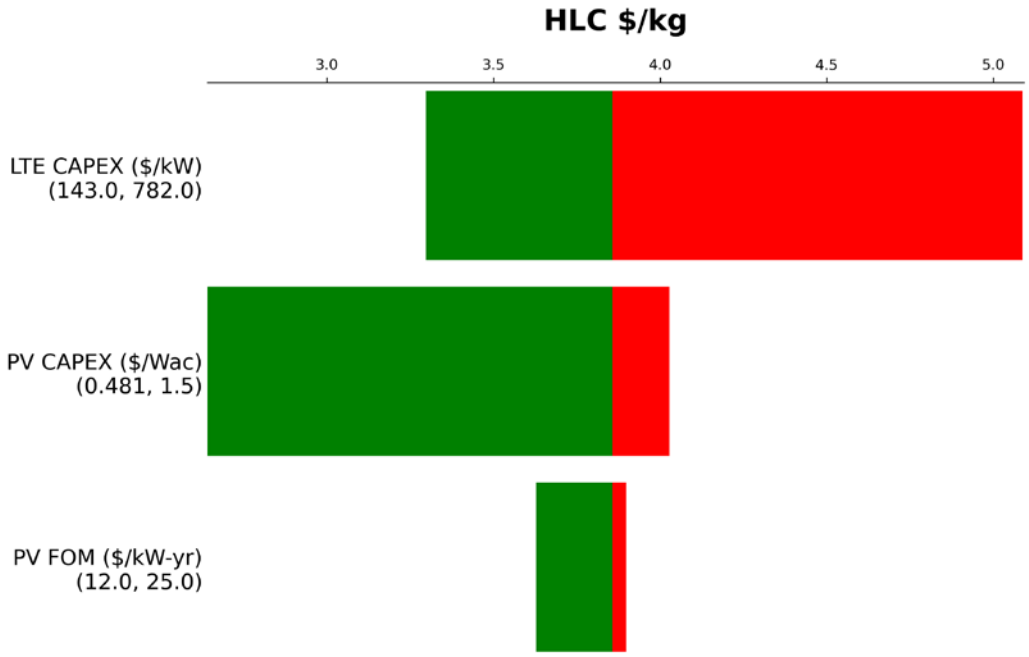

Figure 18. PV-LTE baseline system tornado plot

The contour plot shown in Figure 19 varies the PV and LTE capital costs. This plot is used to identify the parameter space where reductions in both PV and LTE capital costs will result in HLCs below $2/kg H_2. Other parameters that remain constant, such as PV and LTE operating costs, are assumed to be at the 2050 scenario values. The sizes of the PV and LTE components remain constant as well, while in actuality the optimal size ratio is dependent on the relative costs of the two components. However, only a 5 MW difference in LTE size for the baseline 100 MWDC PV size is observed given PV and LTE prices from similar price scenarios. This difference in LTE system size has a relatively minor impact on the hydrogen production cost a per Figure 15. The domain of the contour plot represents expected LTE purchase costs between 2020 and 2050, while the range of the contour plot represents expected utility PV capital costs between a conservative 2020 and advanced 2050 ATB scenario. The circle represents the HLC of the system under the 2020 scenario, while the star represents 2050 scenario. The contour plot shows that the PV-LTE system is unlikely to achieve $2/kg H_2 under conservative cost targets, as the future baseline HLC is $2.13/kg H_2. Reductions in other costs, such as PV and electrolyzer operating costs, PV module efficiency improvements, and LTE stack efficiency improvements, will shift the electrolyzer capital cost for $2/kg H_2 upwards. Another pathway to reduce HLC costs would be adding

battery storage. If the cost of implementing battery storage were low, HLCs could potentially be reduced by utilizing trimmed PV electricity to produce hydrogen.

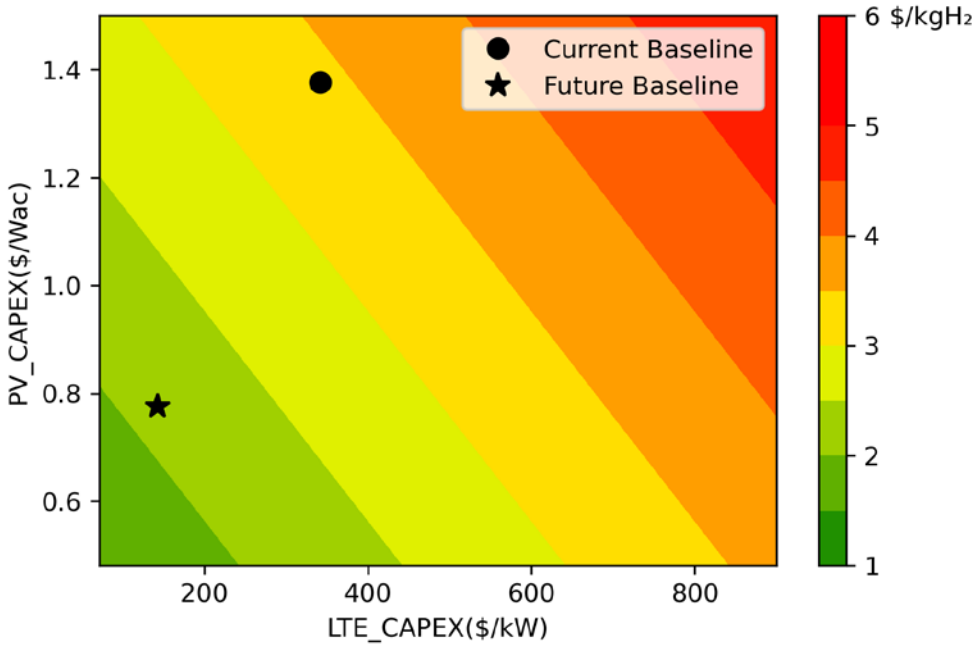

Figure 19. PV-LTE future scenario contour plot that varies the PV capital cost and LTE purchase cost at a constant PV:LTE ratio of 100 MW to 55 MW

Impacts of adding Batteries to PV-LTE systems

The following discussion pertains to the impact of adding batteries to PV-LTE systems. The Li-ion NMC/graphite battery cell model in SAM is used for the utility PV battery storage (DiOrio et al. 2015). Given that the overall system is islanded, the battery is primarily dispatched to store trimmed PV electricity and to discharge trimmed PV electricity when the electrolyzer is underutilized. The two heat maps in Figure 20 show a typical utility battery charge and discharge profile for varying electrolyzer sizes in the baseline case. The top figure represents a 600-MWh and 50-MW battery system coupled to a 100-MW PV array and 55-MW LTE stack. The bottom figure represents the same system but with a 25-MW LTE stack. The 25 MW LTE stack is selected to represent the smaller electrolyzer capacity because a 100 MW PV array can produce 25 MWh of energy each hour averaged over 8760 hours in a year if there was unlimited storage. The battery power and capacity are selected to represent a utility-scale battery system that is sufficient to operate smaller electrolyzers at a higher capacity factor. Section 3.2.1.1 will address trends with regards to different PV-LTE and battery sizing ratios. In the 55-MW LTE case, little electricity is trimmed in the summer daylight hours, which are represented by the light blue-charging profile of the battery. The capacity factor of the electrolyzer marginally increases from 38.5 to 38.8% by adding batteries to the well sized PV LTE configuration. This result is expected as cost optimal sizing minimizes the trimmed electricity and leans towards sizing towards peak summer generation. In the bottom figure, the electrolyzer is significantly smaller resulting in the battery cycling more frequently, which leads to hydrogen production profile that extends over longer hours in a year than the 55-MW case. The capacity factor of the electrolyzer increases from 38.5% to 75.6% as a result of adding batteries. The 12 hours of battery storage in this particular configuration isn't sufficient to capture all the available PV energy as implied by the white section in the afternoon of the summer

months. By comparing the two plots, it is clear that running an electrolyzer at a significantly higher capacity factor requires utility scale battery systems and that there may potentially be an optimal utility scale PV-LTE-Battery configuration that could have a lower hydrogen production cost compared to the baseline PV-LTE system. To that end, several questions below need to be addressed.

- What battery-electrolyzer-PV combination would result in lower, or more competitive, HLC than the optimal storage-less PV-LTE configuration?
- What battery capital costs enable PV-LTE-battery configurations to be cost competitive with the baseline PV-LTE system. At what capital cost will adding batteries always be competitive from a HLC perspective?
- When does replacing LTE capacity with battery capacity to produce hydrogen at a more constant load make sense?

These questions are investigated in this report by doing a parametric study on adding batteries to PV-LTE systems.

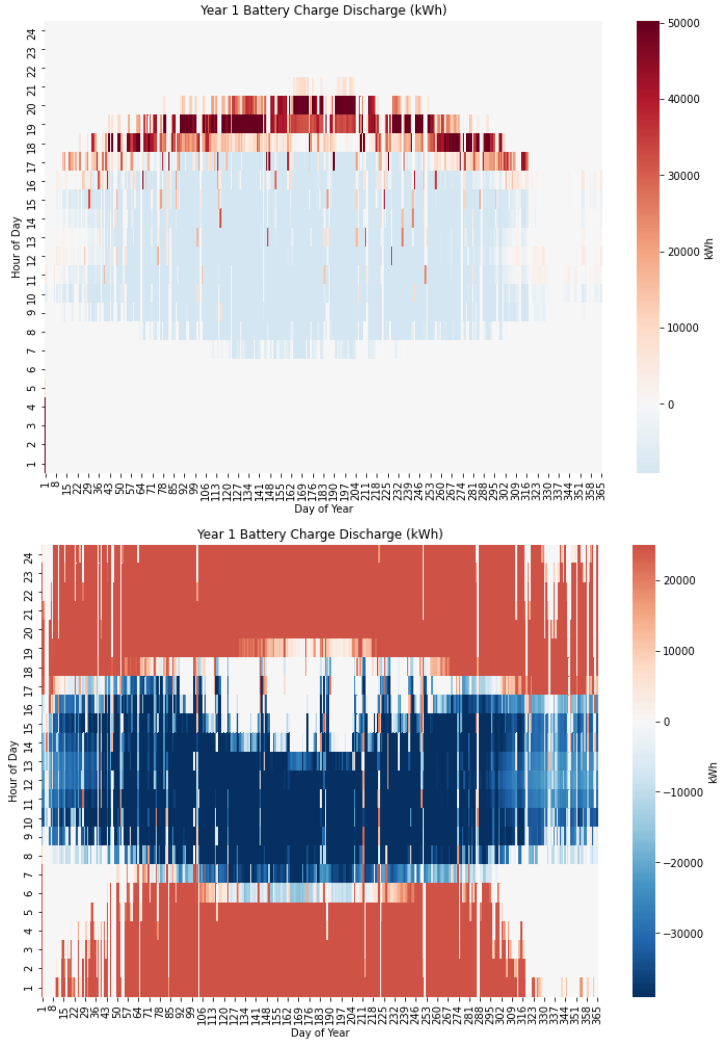

Figure 20. Battery charge and discharge profiles for a 600 MWh/50 MW Li-ion battery coupled to a 100-MW PV array and 55-MW LTE (top figure) and 25-MW LTE (bottom figure)

3.2.1.1 Technoeconomic Analyses of adding Batteries to PV-LTE systems via a Parametric Study

Because of the lack of hybrid optimization in the current SAM version, the initial approach to explore this problem was to employ a parametric analysis. The parameters varied are presented in Table 15. The battery power and hours of storage are varied among the typical utility-scale battery values found in the ATB. The battery capital cost range represents the DOE Earthshot, Storage target of 10% up to current battery costs (100%) ("Long Duration Storage Shot: An Introduction" 2021). All other parameters such as PV system performance and costs, LTE efficiency are assumed to be at 2050 scenario values.

Table 15. Battery Parametric Simulation Input Parameters

Parameter	Values
Battery Power (MW)	1, 10, 50
LTE Purchase Cost ($/kW)	143, 342, 782
LTE System Size (MW)	25, 30, 35, 40, 45, 50, 55
Hours of Battery Storage	4, 8, 12
Battery Capital Cost (% of current)	10, ATB 2040 Advanced, ATB 2030 Moderate, ATB 2020 Conservative

ATB = Annual Technology Baseline

The goal of the parametric study was to identify cases where adding batteries resulted in lower, or more competitive, HLCs than the optimal storage-less PV-LTE system. The first set of plots in Figure 21 exclusively covers the cases where the battery system capacities are 50 MW and 600 MWh and are added to a 25-MW LTE for the 100-MW PV array. In this utility-scale battery case, the objective is to reduce the HLC and extend the number of production hours. Each subplot represents a particular stack purchase cost. The solid lines represent the optimal HLC without battery storage at that purchase cost, and the dots represent the HLC at various battery configurations.

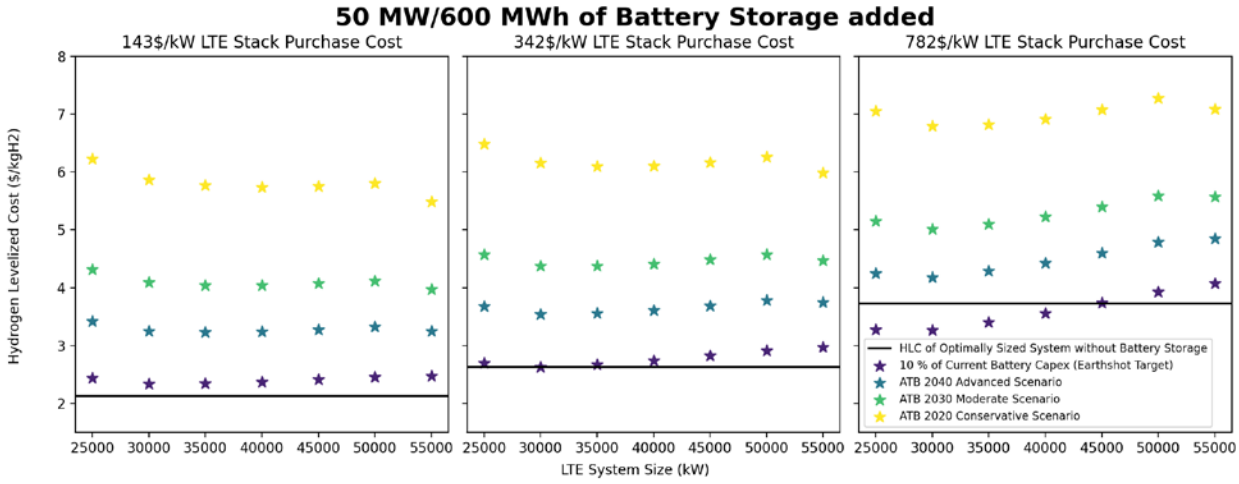

Figure 21. Battery parametric simulation results that highlight the impact of battery capital costs, relative to LTE capital costs, on the potential to reduce HLCs for utility-scale battery storage

At LTE costs of $143/kW, the optimal HLC for a storage-less system is lower than all of the battery configurations added to the PV-LTE system. Cheap electrolyzer capacity reduces the need for batteries

from a minimum HLC perspective. The electrolyzer capacity has a significant impact on the HLC when the electrolyzer is undersized and has a diminishing impact as the capacity approaches the optimal range of 50–60 MW for the 100-MW PV system. Battery costs also significantly affect the HLC, as battery costs that achieve the Earthshot, Long Duration Storage Shot targets result in HLCs that are up to $ 4/kg H_2 lower than the HLC using current battery costs. When the electrolyzer stack purchase cost increases, systems with battery storage have increased competitiveness as the costs of battery versus stack begin to decrease. At current stack costs of $782/kW, a band of undersized LTE with utility-scale battery storage systems has significantly lower HLCs or is competitive with storage-less systems. At $342/kW, several configurations remain competitive with storage-less systems.

The rule-of-thumb cutoff for when battery storage is competitive with storage-less systems is $342/kW stack purchase costs requiring battery capital cost reductions of 90%, and $782/kW stack purchase costs requiring at least battery capital cost to achieve ATB 2040 advanced scenario targets. The hydrogen production profile for the 25 MW LTE with a battery system of 50 MW/600 MWh case at the $782/kW stack purchase cost is shown in Figure 22. For most of the year, the system produces hydrogen at 12–20 hours per day.

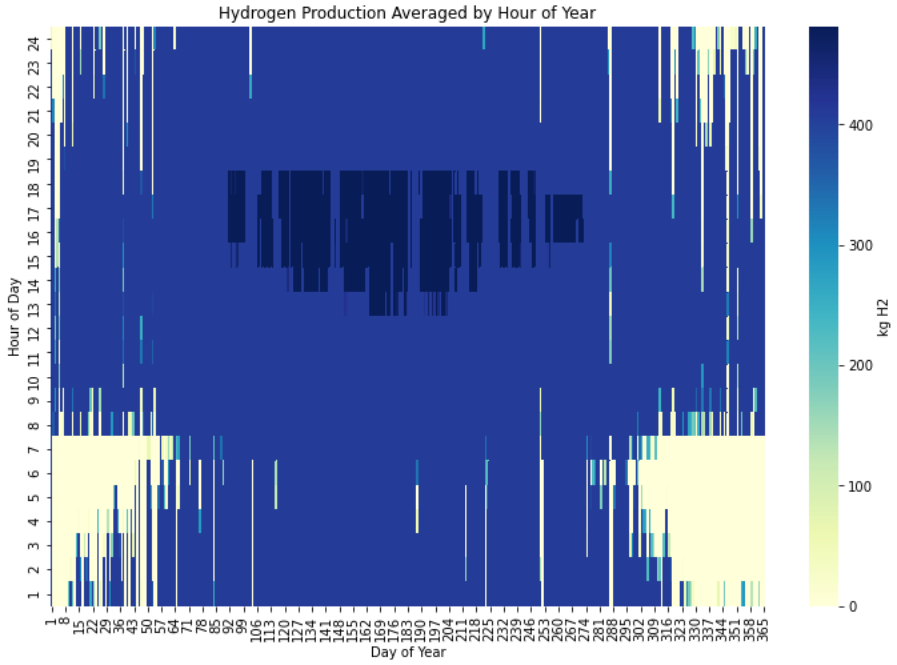

Figure 22. Hourly hydrogen production profile for a 25-MW LTE coupled to a 50 MW/600 MWh battery and 100 MW PV system

3.2.1.2 Lowest HLC PV-LTE-Battery Systems

The lowest HLC of every PV-LTE-Battery configuration is presented in Figure 23 as a function of the LTE system size and battery cost scenario. Where colored stars are missing, such as the case of a 35-MW LTE for a stack purchase cost of $143/kW, the HLC at that point does not use battery storage as no sensitivity occurs in changing the storage cost scenario. The only parameter space where battery storage improves the HLC of the PV-LTE system is where the LTE stack purchase costs are $782/kW and the battery costs are 90% of current costs ("Long Duration Storage Shot: An Introduction" 2021). In addition, when the stack purchase cost is $782/kW, battery configurations using ATB 2040 advanced

costs are also competitive with the optimal storage-less PV-LTE system. When the LTE purchase costs decrease to $342/kW and $143/kW, only PV-LTE-Battery configurations under the DOE Earthshot assumptions remain cost competitive with the optimal storage-less PV-LTE system.

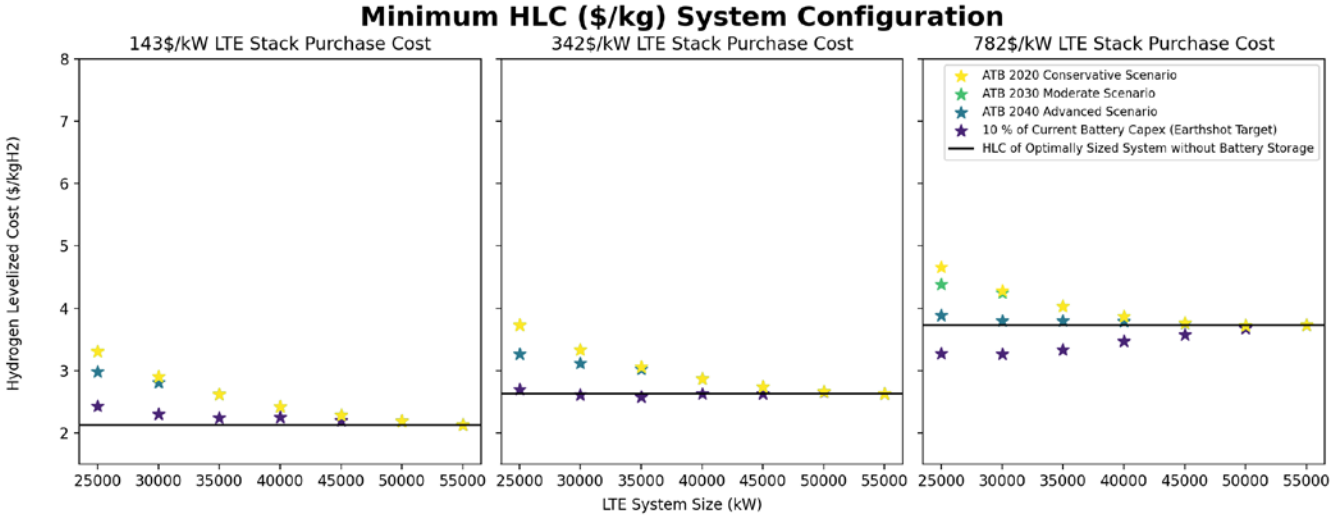

Figure 23. Lowest HLC battery configuration for each battery capital cost, LTE system size, and LTE capital cost combination

The lowest HLC PV-LTE-Battery configuration for the Earthshot/ATB 2040 advanced scenario and stack purchase cost in Figure 23 is presented below in Table 16. The ATB 2020 and 2030 battery cost scenarios are not included as they are not competitive with the cost-optimal PV-LTE system without batteries with LTE purchase costs $342/kW and below. As expected, the only cases where adding battery storage improves the HLC is under the DOE Earthshot, Long Duration Storage Shot battery cost scenario at the $782/kW and $342/kW stack purchase costs. The HLC improves from $3.73 to 3.27/kg H_2 by adding a 50 MW/400 MWh battery to a 25 MW LTE when the stack purchase cost is $782/kW. The HLC improves from $2.62 to 2.57/kg H_2 by adding a 25 MW/300 MWh battery to a 35 MW LTE when the stack purchase cost is $342/kW. In all other cases the battery configuration with the lowest HLC is the smallest possible battery in the parametric study. This implies that it isn't cost optimal to add batteries in those particular scenarios.

Under DOE Earthshot battery costs and a $143/kW stack purchase cost, the LTE capacity of a lowest HLC PV-LTE-Battery configuration with a 50 MW/600 MWh battery is 30 MW. The HLC of this particular configuration is $2.34/kg H_2 which is approximately 10% higher than the baseline HLC of $2.13/kg H_2. Running a higher capacity factor electrolyzer using utility-scale batteries is still competitive when the stack purchase cost is low. However, whether this system is economically feasible will ultimately depend on hydrogen threshold price of the end user and the associated benefit with a more steady supply of H_2 by adding a battery. None of the PV-LTE battery configurations achieve the HLC target of $2/kg H_2.

Table 16. Lowest HLC Battery Configurations within the Parametric Study

Battery Cost Scenario	Stack Purchase Cost ($/kW)	LTE Capacity / Battery Power /Hours of Storage / Electrolyzer Capacity Factor	HLC (kg H_2)
PV-LTE Baseline without Storage	782	55 MW / 0 MW / 0 hours / 38.8%	3.73
	342		2.62
	143		2.13
DOE Earthshot	782	25 MW / 50 MW / 8 hours / 75.9%	3.27
	342	35 MW / 25 MW / 12 hours / 58.8%	2.57
	143	55 MW / 1 MW / 4 hours / 38.8%	2.13
ATB 2040 Advanced	782	55 MW / 1 MW / 4 hours / 38.8%	3.73
	342	55 MW / 1 MW / 4 hours / 38.8%	2.64
	143	55 MW / 1 MW / 4 hours / 38.8%	2.14

3.3 System 3: MSALT-HTSE – Hybrid Tower and HTSE

A block flow diagram of the hybrid molten salt tower coupled to an HTSE system is presented in Figure 24. The salt flow is split to provide heat for the HTSE through feedwater vaporization as well as heat for the power block to produce electricity. The overall system is dispatched to meet a constant load, as HTSEs typically are not load-following and generally prefer to be run constantly at nominal capacity.

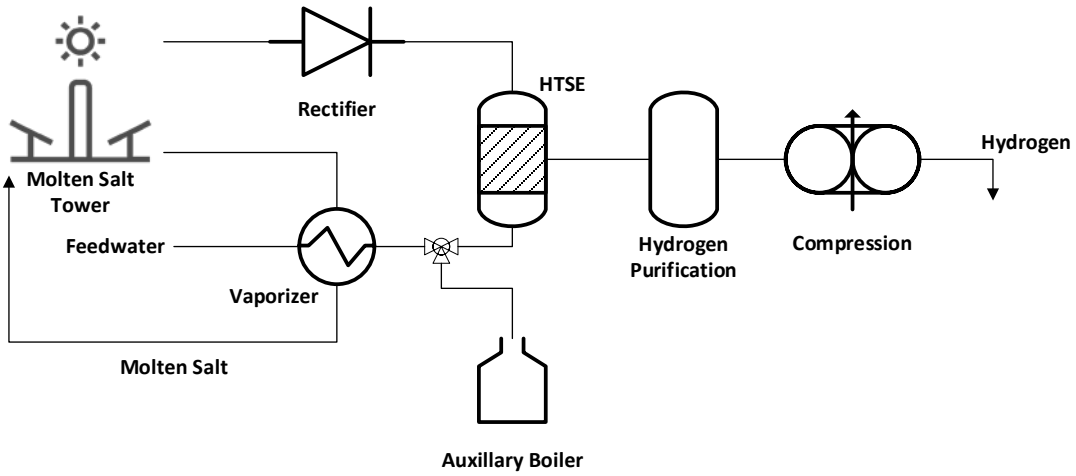

Figure 24. MSALT-HTSE system block flow diagram

Using this tower model, a grid search is conducted to size the individual subcomponents and parameters of the overall system. Specifically, the heat output for a constant electrical tower capacity and the nominal HTSE system size are both varied to identify the parameter values at which the HLC would be minimized for the overall system. The results of the grid search are shown in Figure 25. For a fixed 115-MWe tower, the optimal heat capacity of the salt flow to the feedwater vaporizer is between 21 MWth and 24 MWth. Sensitivity to the additional heat capacity devoted to supplying heat to the HTSE is significant, especially for large HTSE system sizes. Undersized heat capacities can account for $0.5/kg H_2 as the electrical output of the tower becomes the limiting energy input for HTSE hydrogen

production. Conversely, oversized tower heat capacities do not affect the HLC as much as undersized heat capacities, as indicated by the darker blue region in the top right corner of Figure 25.

Electricity is more expensive to produce than heat; increasing the tower electrical output would require increasing both the tower and power block capacities, while increasing the heat capacity would only influence the tower capacity. Thus, when an HTSE is coupled to a hybrid tower, ensuring that the heat component is the limiting energy input to the HTSE is economically favorable. If the heat and electricity are sufficient, the size of the HTSE system does not significantly affect the overall HLC of the system, as the HTSE system costs are an order of magnitude below tower costs. An optimal baseline HLC of \$3.93/kg H_2 is obtained for a 115 MWe/22 MWth tower coupled to a 115-MW HTSE system.

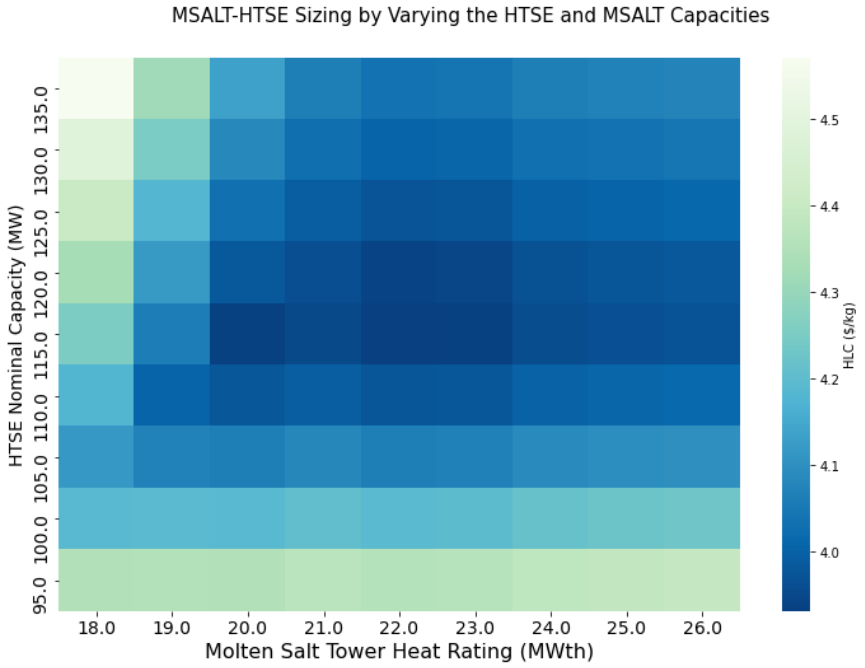

Figure 25. MSALT-HTSE System Grid Search Sizing Results

The overall system production ranges from 20 hours of near-constant hydrogen in the summer months to 12 hours of hydrogen in the winter months with 10 hours of thermal energy storage, as shown in Figure 26. This system is the only baseline system explored in this report that can reach constant load hydrogen production over the course of 20 hours, as thermal salt storage is significantly cheaper than lithium-ion battery storage on a per-kWh basis. This system is more economically viable than both of the PV-based systems to provide a constant load to longer operating schedules, as both PV systems would need to turn down the hydrogen production rate at night hours because of the limitations of battery power on storage. The overall HTSE capacity factor for the baseline system described is 58.4%.

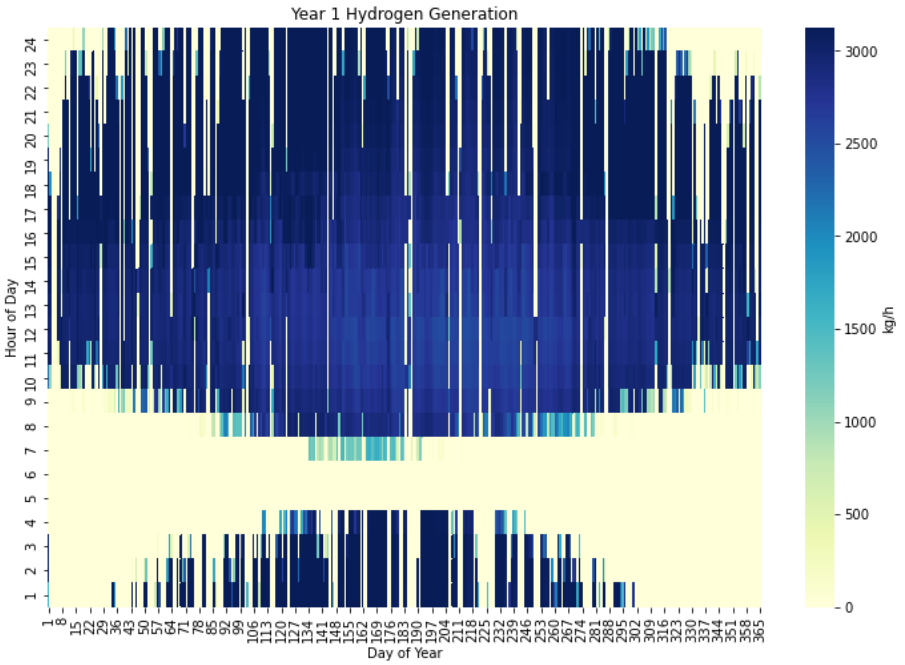

Figure 26. Year 1 baseline MSALT-HTSE hydrogen production heat map

Standby and parasitic loads occur as the tower cannot provide both heat and electricity constantly for the entire day, especially in the winter months. The graphs in Figure 27 show the typical electricity (lefthand graph) and heat (righthand graph) inputs, respectively, required to meet tower parasitic loads and HTSE hot standby requirements. The minimum turbine fraction limits the ability of the tower to dispatch to meet the parasitic loads.

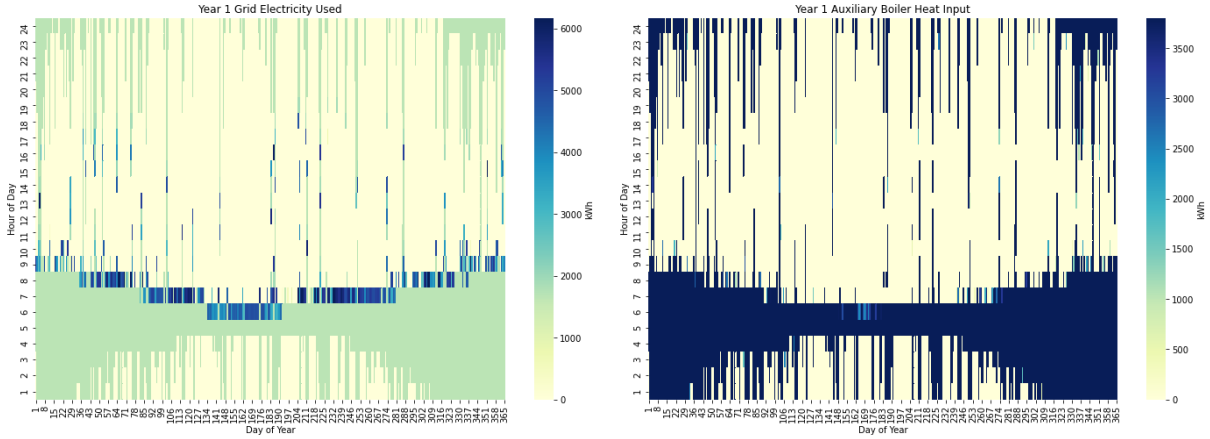

Figure 27. Grid electricity consumption (left) and boiler heat input (right) required to operate the baseline MSALT-HTSE system

The current 2020 baseline value of \$3.93/kg H_2 for this system is significantly above the target HLC of \$2/kg H_2. Tornado and contour plots, similar to those created for the PV-LTE system, were developed to identify the parameter space where the HLC of the hybrid tower coupled to the HTSE could approach \$2/kg H_2. Figure 28 highlights the key parameters that influence the tower cost.

The tower capital cost is the main parameter that influences the overall HLC of the system, with HTSE capital cost being the second-most sensitive parameter related to reducing the HLC. Reducing the storage from 10 hours to 8 hours has a higher impact on the HLC than increasing the HTSE uninstalled cost from $425/kW to $522/kW; however, increasing the amount of storage from 10 hours to 12 hours does not improve the HLC substantially. The baseline HLCs at 8, 10, and 12 hours of storage are $4.06, $3.93, and $3.91/kg H_2, respectively. The minute differences between HLCs at varying storage hours exceeding 10 hours make drawing a conclusion difficult because of the overall error bars of the simulation. The key conclusion is that the hybrid tower should have at least 10 hours of thermal storage when coupled to an HTSE, with the exact number of hours depending on the hydrogen demand curve for a particular end use.

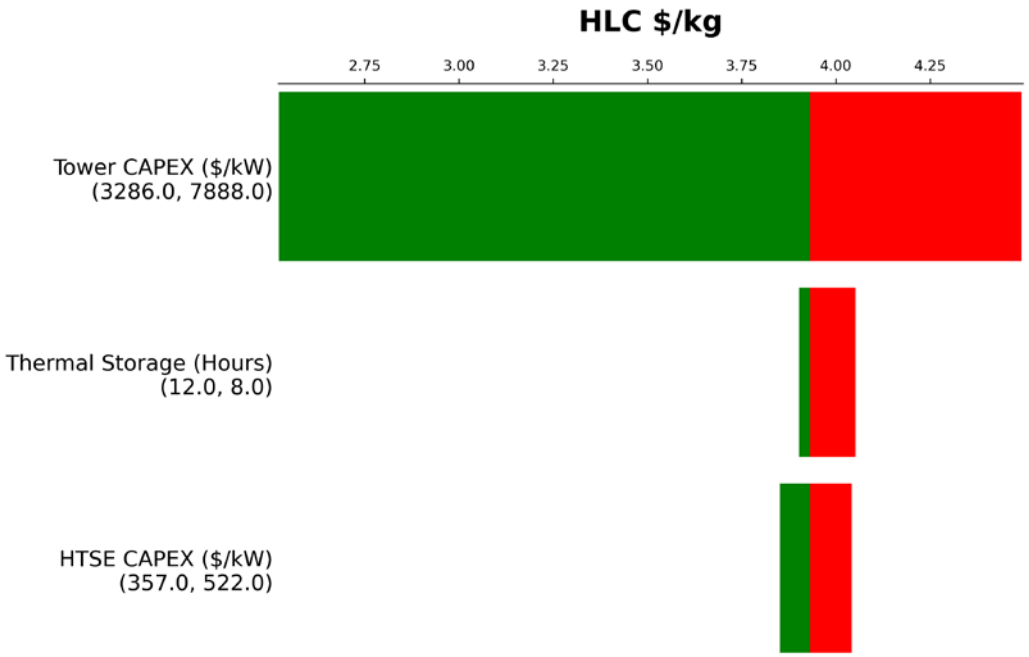

Figure 28. Baseline MSALT-HTSE system tornado plot

A contour plot that varies the tower and HTSE capital costs was used to identify the parameter space where $2/kg H_2 could be achieved, as shown in Figure 29. Given the current advanced ATB tower cost projections for 2050 and DOE 2050 HTSE program record costs, this system will be unlikely to achieve $2/kg H_2. The future baseline value is $2.84/kg H_2, while advanced ATB tower projections would bring the HLC down to approximately $2.30/kg H_2, which is represented by the forest green section of the plot in Figure 29.

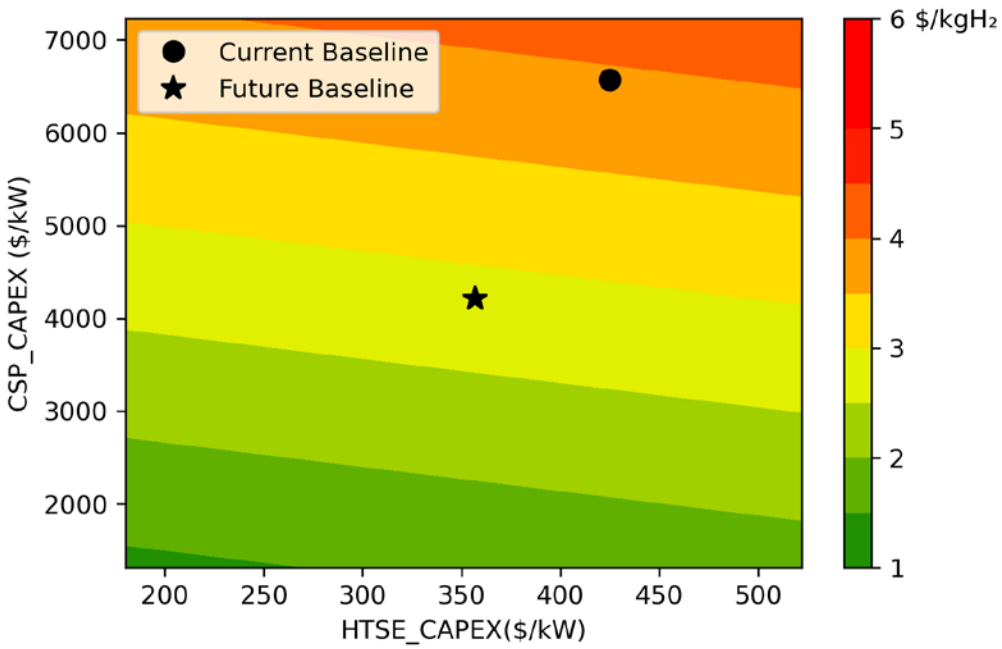

Figure 29. Baseline MSALT-HTSE system contour plot for Daggett, California, with an extended domain and range to show the $2/kg H_2 regime

3.4 System 4: PV-MSALT-HTSE – PV, Heat Tower, and HTSE

A block flow diagram of the PV, heat-only tower, and HTSE configuration is presented in Figure 30. The baseline system does not include battery storage coupled to PV. The tower thermal storage is dispatched to match the AC output of the PV system in the amount required by the HTSE. The overall system is islanded except for a small grid connection and auxiliary boiler to maintain the HTSE at hot standby.

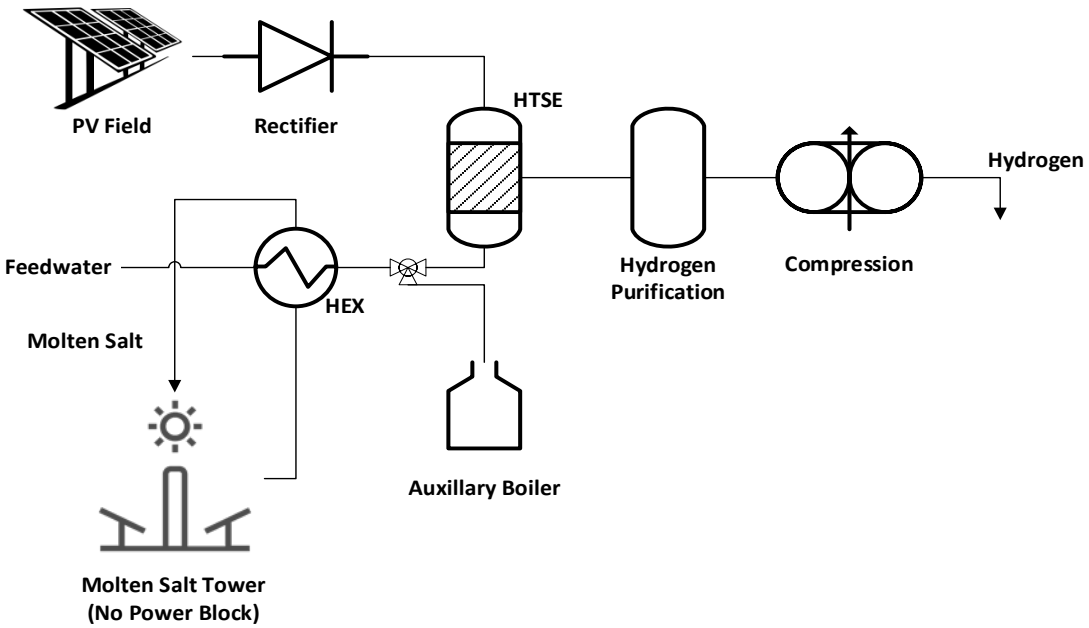

Figure 30. PV-MSALT-HTSE system block flow diagram

In an approach similar to the MSALT-HTSE system, a grid search was conducted to identify the cost-optimal system configuration for PV-MSALT-HTSE, as shown in Figure 31. The HTSE system capacity and tower thermal capacity are varied for a fixed 100-MWe PV system. Unlike the MSALT-HTSE system, cost sensitivity is significant for both the tower heat capacity and HTSE nominal capacity. The optimal HLC is a 15-MWth tower and 100-MWe PV coupled to a 60-MW HTSE. The HLC for this baseline system is \$2.90/kg H_2, which is significantly lower than the baseline HLCs for the prior two systems. The primary drivers of the reduced costs are the relatively cheap PV, lower costs for smaller towers, and a higher-efficiency and lower-cost HTSE system compared to the LTE system.

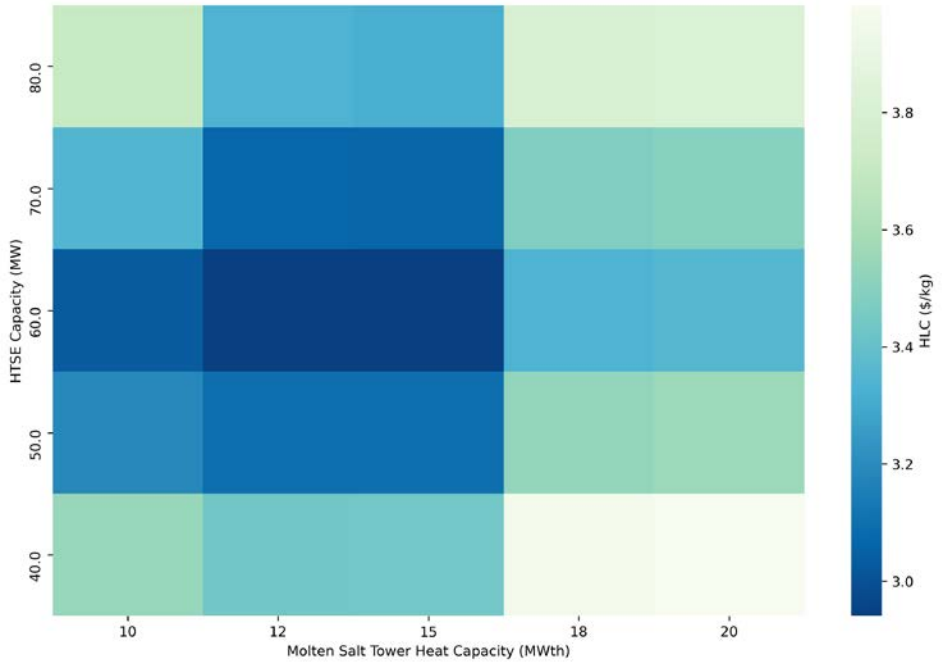

Figure 31. PV-MSALT-HTSE system sizing results

As mentioned previously, the tower thermal storage is used to dispatch the tower heat output to align with PV generation, to the extent possible. In addition, heat from the tower is used for the HTSE hot standby requirement, which is 19% of the nominal HTSE thermal load. Batteries could be added to the PV system to meet HTSE hot standby electrical loads; however, only a small battery of approximately 1 MW with 10–12 hours of storage would be required, as the HTSE hot standby electrical load is 0.9% of the nominal value. Electrical loads (parasitic or standby) that are unmet by PV generation are currently captured by a small grid connection. The two profiles in Figure 32 highlight the PV (top image) and heat (bottom image) energy generation in the first year for this system.

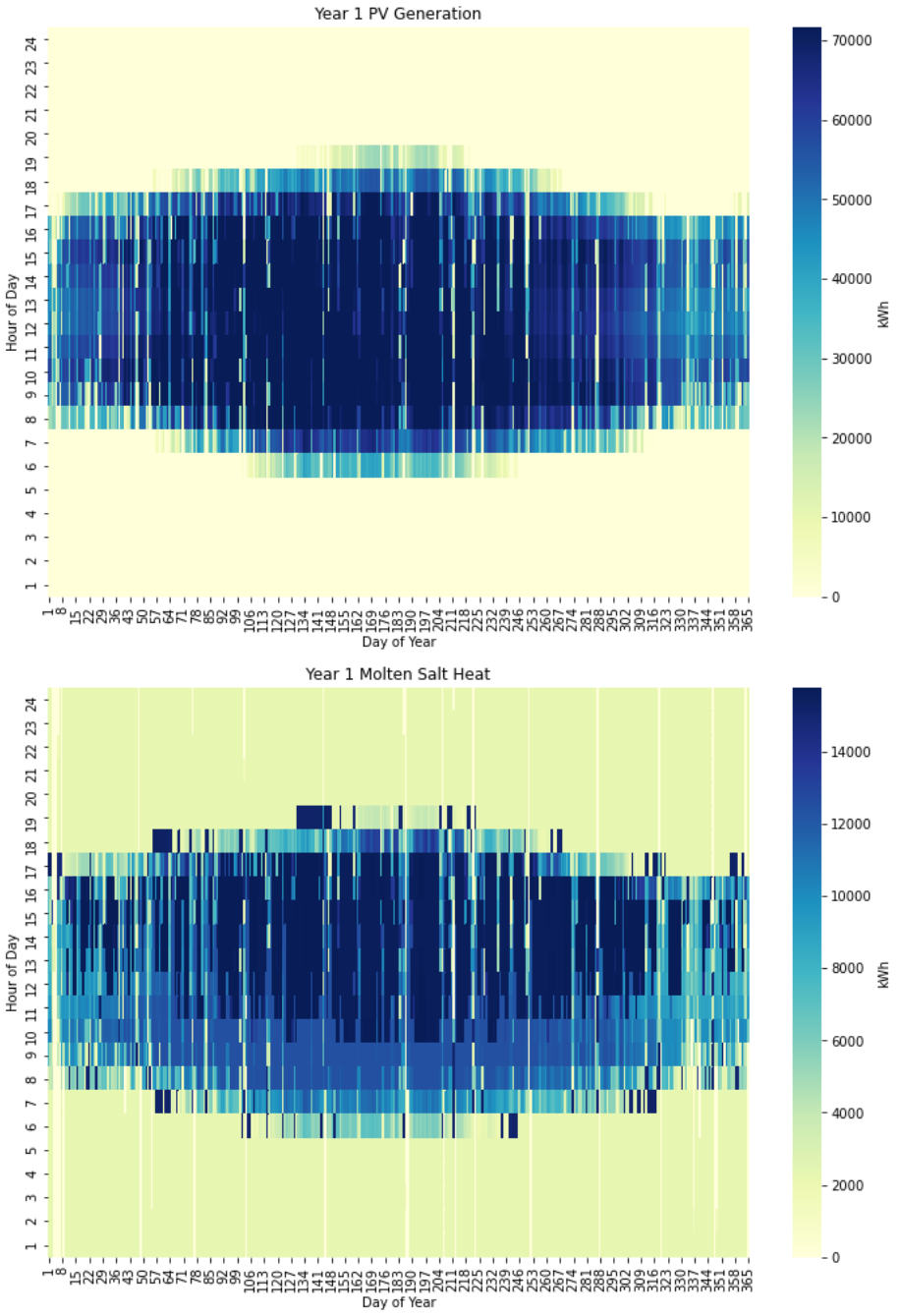

Figure 32. PV generation in Year 1 (top image) and dispatched tower heat generation in Year 1 (bottom image)

The current 2020 baseline value of \$2.90/kg H_2 is approaching the target HLC of \$2/kg H_2. Figure 33 highlights the key parameters that affect the overall system HLC. The main cost driver for PV-MSALT-HTSE is the PV capital cost, which varies between the 2020 and 2050 conservative ATB scenario values. Reducing the PV fixed annual operating cost from \$23/kw-yr to \$10/kw-yr provides a greater cost reduction than the HTSE CAPEX, highlighting the dependence of the HLC on the PV system size. Neither of the major cost drivers can reduce the HLC to \$2/kg H_2; a combination of cost reductions would be required to achieve \$2/kg H2.

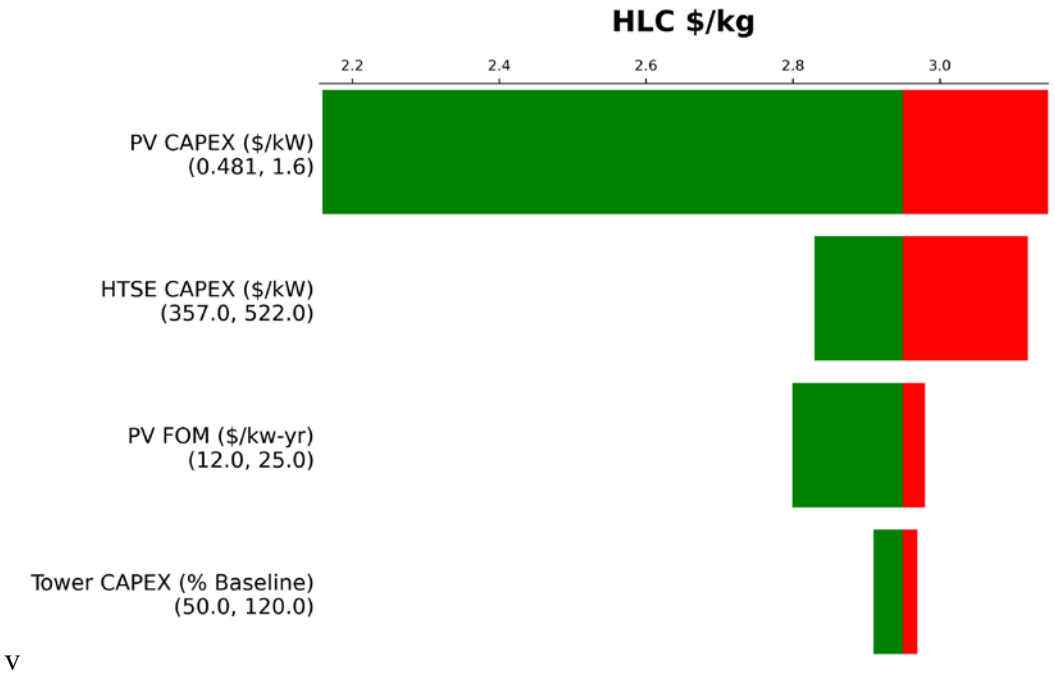

Figure 33. Baseline PV-MSALT-HTSE system tornado plot

A contour plot is used to explore conditions under which \$2/kg H_2 is achieved. Although the PV-MSALT-HTSE system has the lowest HLC in the 2020 scenario, the system is unable to achieve \$2/kg H_2 given the 2050 projections of PV and HTSE costs, as shown in Figure 34. An HLC of \$2.13/kg H_2 is obtained at future baseline values, as indicated by the star in the figure. The contour plot is extended using more optimistic values than 2050 projections to give insight into the HTSE capital cost and PV capital cost combinations that would result in \$2/kg H_2 in Figure 35.

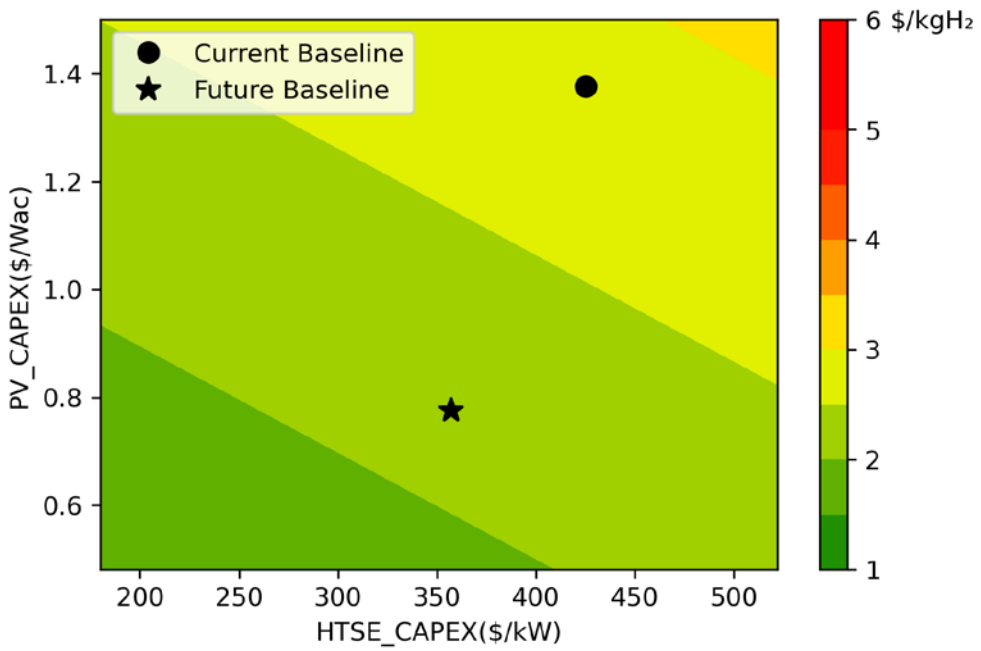

Figure 34. Baseline PV-MSALT-HTSE contour plot varying the PV capital cost and the HTSE capital cost for future projections (star) and with the axes extended to highlight the $2/kg H_2 regime

3.5 Location-Wide Analysis

Forty locations in the United States are used in a solar-hydrogen potentials analysis within this section to identify trends in system HLCs and designs. Each system is compared for various locations. The overall analysis highlights when and where solar hydrogen systems can be deployed to produce hydrogen at $2/kg H_2, as well as which system will most likely be the frontrunner from an HLC perspective. The general simulation steps for the United States potentials analysis are as follows:

1. Select a location, scenario (i.e., 2020 versus 2050), and system.
2. Update location-sensitive parameter values, such as the weather resource file, electricity prices, and natural gas prices.
3. Size the system at the selected location.
4. Calculate the HLC at the selected location using the optimal system configuration.

The optimal system subcomponent size for the baseline systems was calculated for each location and system. The general conclusion was that the system subcomponent sizes had very little variability, even with the significant variability in solar resources at each location. For the PV-LTE system, the optimal system size for the 2020 scenario varies between 50 MW and 55 MW for a 100-MWe PV system, with 55-MW LTEs being optimal for higher solar resource locations. Figure 35 shows the optimal system size for each location for the PV-LTE system.

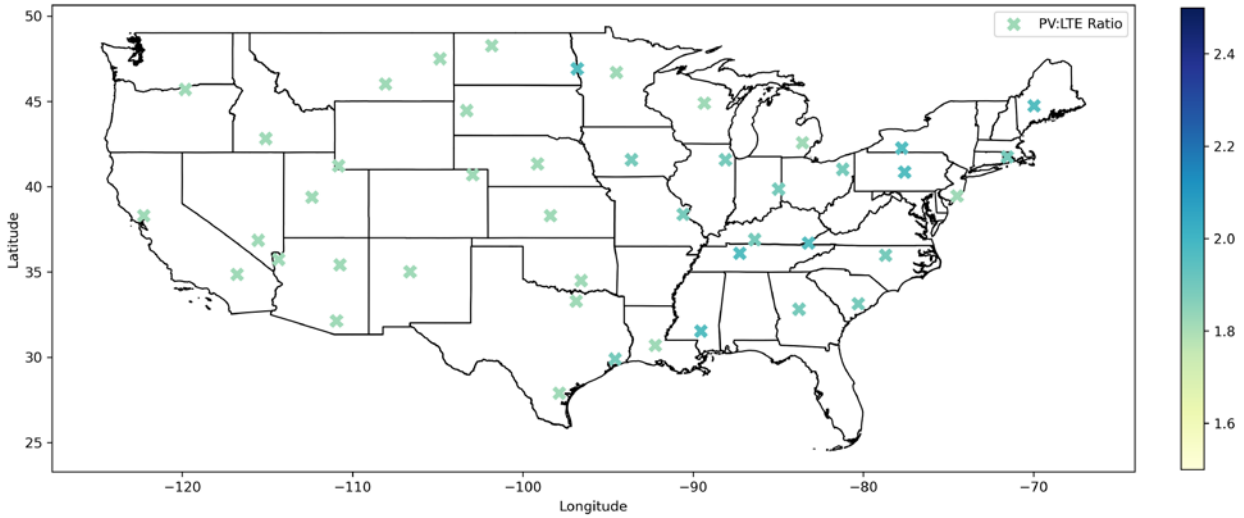

Figure 35. PV-LTE capacity ratio across all U.S. locations for the 2020 scenario

The system with the lowest HLC in the 2020 scenario is plotted for each location in Figure 36. PV-MSALT-HTSE has the lowest HLC in all locations, considering the cheaper and more efficient HTSE relative to the LTE in 2020, as well as the lower-cost PV. As expected, the regions of the United States with higher solar resources have the lowest HLCs, with differences being close to 50% of the HLCs in poorer-resource locations. Because the PV-MSALT-HTSE system is unable to meet \$2/kg H_2 using the current 2050 cost projections for PV and HTSE capital costs in very high solar resource locations, PV-MSALT-HTSE is unlikely to be deployed to produce hydrogen in regions outside the Southwestern United States.

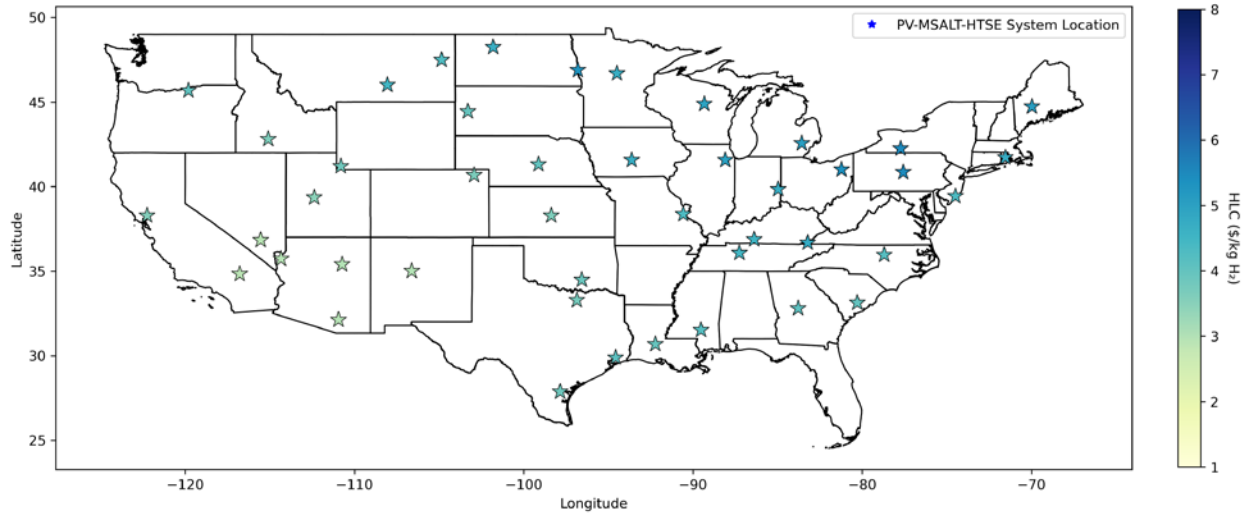

Figure 36. The lowest HLC system for the 2020 scenario is the PV-MSALT-HTSE system in all U.S. locations

In 2050, PV-LTE becomes the lowest cost hydrogen production system in all regions as shown in Figure 37. This improvement in competitiveness is driven by significant reductions in LTE stack purchase costs from \$342/kW to \$143/kW compared to the HTSE system cost reduction of \$425/kW to \$357/kW. In this 2050 scenario, HLCs approach in \$2/kg H_2 exclusively in the southwest United States. Other regions in the U.S. have HLCs between \$2.5/kg H_2 up to \$4/kg H_2 at New York. Even with significant

PV and LTE cost reductions, \$2/kg H_2 is not reached for a significant portion of the continental United States.

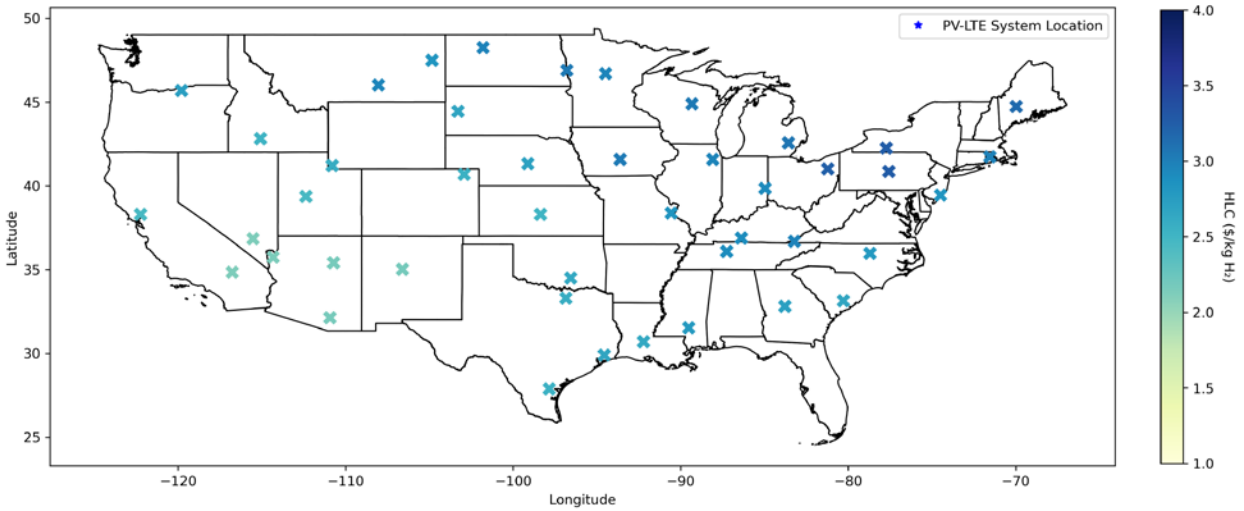

Figure 37. The lowest HLCs system for the 2050 scenario is the PV-LTE system in all U.S. locations

The competitiveness of PV-LTE compared to PV-MSALT-HTSE changes between 2020 and 2050. At an intermediate cost and performance, PV-LTE begins to have a competitive HLC in regions with lower solar resources. Figure 38 provides an intermediate case where the LTE cost is \$300/kW and the HTSE and PV costs remain at the 2050 values. The color represents the % difference between the HLCs of the two systems. A blue color represents locations where PV-MSALT-HTSE systems are cheaper than PV-LTE systems while red represents locations where PV-MSALT-HTSE systems are more expensive than PV-LTE systems. At a \$300/kW LTE cost, the lowest-cost system in regions outside of the Southwest begins to move from the PV-MSALT-HTSE system to PV-LTE.

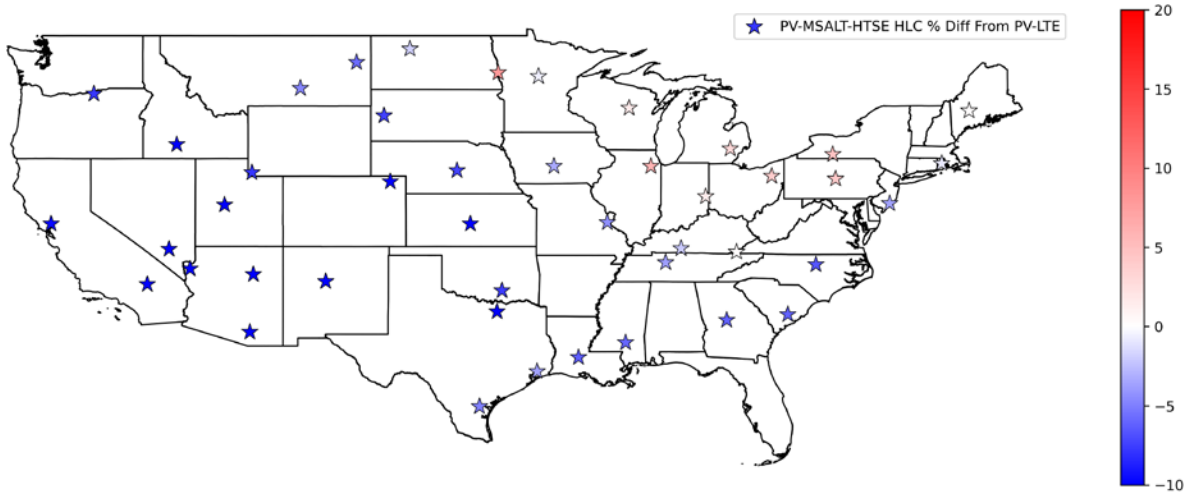

Figure 38. The PV-MSALT-HTSE percentage differences from PV-LTE systems at a \$300/kW LTE purchase cost with all other parameters at 2050 scenario values

While objectively the PV-LTE system is the lowest cost system in the 2050 scenario, there isn't a significant difference in HLCs between PV-LTE and PV-MSALT-HTSE systems in the southwest U.S. region where PV-MSALT-HTSE systems are competitive. Figure 39 below how the % difference

between the HLCs of the two systems in the 2050 scenario. PV-MSALT-HTSE HLCs are 1% to 22% higher than PV-LTE systems. Given that a 1% HLC difference is well within the margin of error of the assumptions used in the simulations, PV-MSALT-HTSE systems are a viable centralized hydrogen production configuration in the 2050 scenario alongside PV-LTE systems. Given that PV-MSALT-HTSE systems are also the only electrolytic hydrogen system competitive with grid electrolysis in the 2020 scenario, one could argue that it is most likely out of the four systems analyzed to be cost competitive with conventional hydrogen production or grid electrolysis regardless of whether future projections are met.

Figure 39. The PV-MSALT-HTSE percentage differences from PV-LTE systems in the 2050 scenario

As mentioned previously, only PV-LTE systems in 2050 reach \$2/kg H_2, provided that R&D is very aggressive, while no system achieves \$2/kg H_2 given current projections. The value of the key cost driver for each system to reach \$2/kg H_2 was determined for each location. Figure 40 shows the capital cost of the PV system required to reach \$2/kg H_2 in 2050. Multiple locations in the Southwest can achieve \$2/kg H_2 given moderate R&D and PV capital cost targets of \$0.65/WAC. With aggressive R&D and PV capital costs of \$0.50/WAC in 2050, some locations in the Midwest would approach \$2/kg H_2. The \$2/kg H_2 target is unlikely to be achieved in the Eastern United States without PV capital costs approaching \$0.20/WAC.

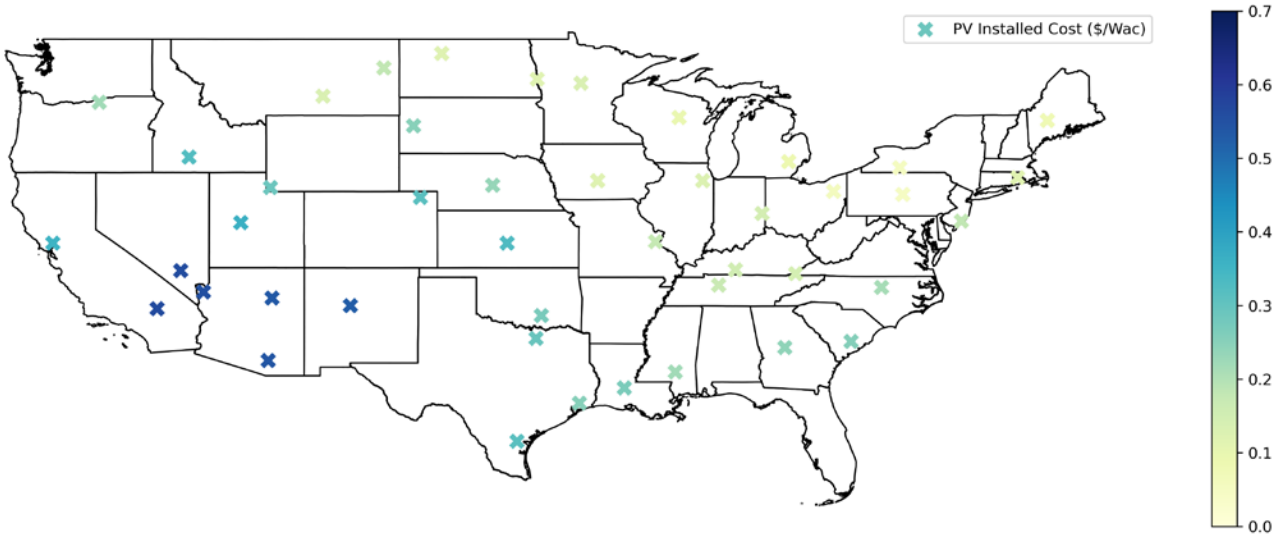

Figure 40. PV capital costs needed to achieve $2/kg H_2, given 2050 scenario projections for the PV-LTE system

Hybrid salt tower capital costs of $2,000/kW in 2050 result in HLCs of $2/kg H_2 in the high solar resource locations, which is well below the aggressive R&D capital cost targets of $2,743/kW for salt towers. In regions with lower solar resources, tower costs alone would be unlikely to result in HLCs of $2/kg H_2 as seen in Figure 41 below.

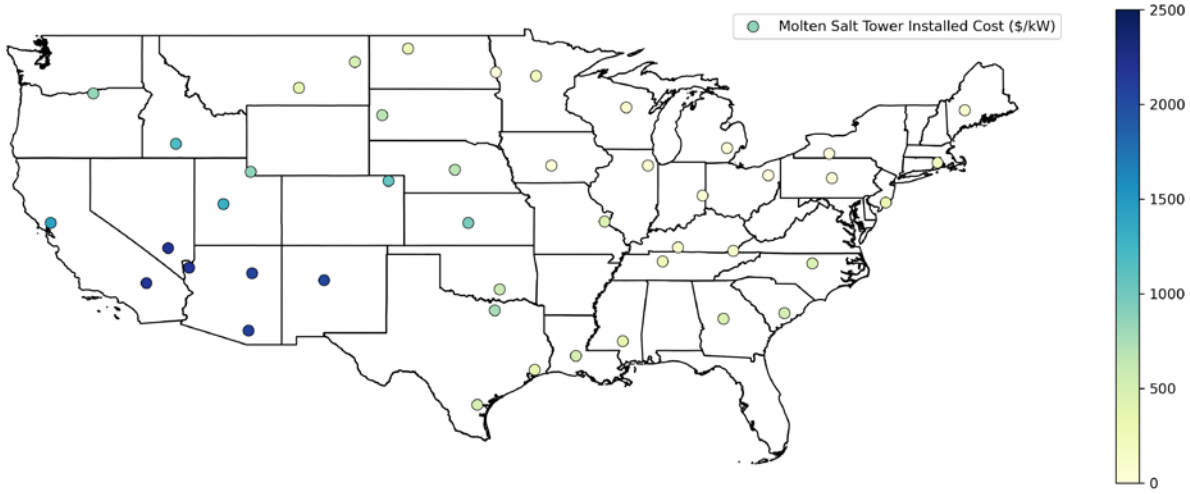

Figure 41. Molten salt tower installed costs needed to achieve $2/kg H_2 given 2050 scenario projections for the MSALT-HTSE system

The PV-MSALT-HTSE system can achieve $2/kg H_2 with PV capital costs of $0.50 to $0.70/WAC, which is similar to the PV-LTE systems as seen in Figure 42 below. In locations with poorer solar resources, however, PV-MSALT-HTSE performs poorly because of limited hours of solar energy, which impacts the salt tower. Having 10–12 hours of thermal storage in a low solar resource location is insufficient to properly dispatch the tower to match PV generation, resulting in significantly higher HLCs that cannot approach $2/kg H_2.

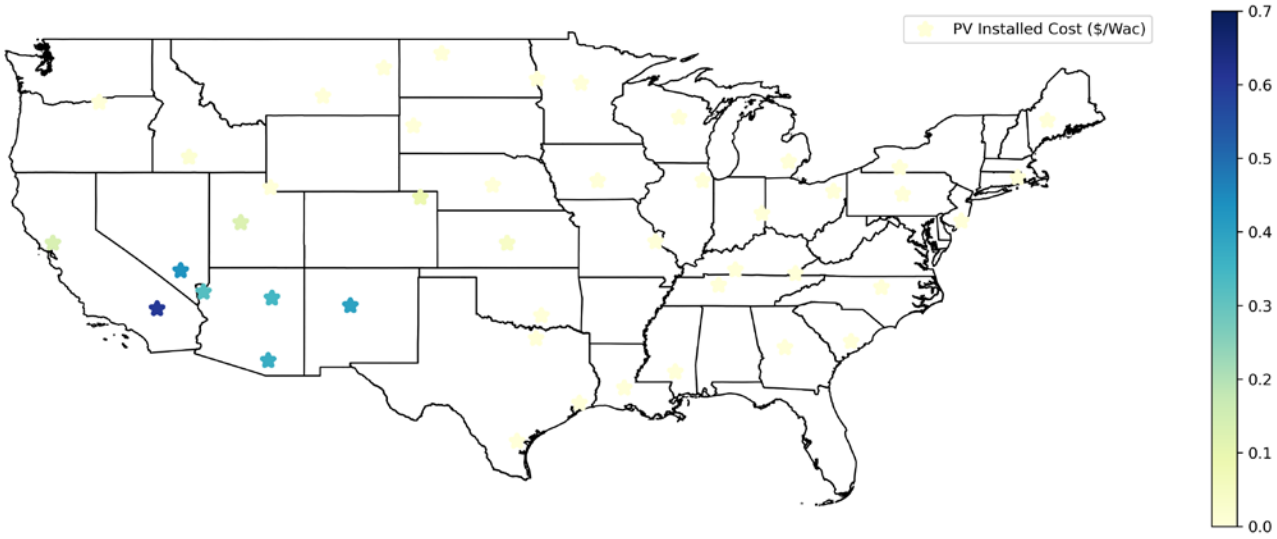

Figure 42. PV capital costs needed to achieve $2/kg H_2, given 2050 scenario projections for the PV-MSALT-HTSE system

4 Conclusions

This section discusses our findings on whether solar H_2 can be competitive with Grid-LTE systems in the future time frame and compete with standard centralized hydrogen production systems. This initial analysis indicates that $2/kg H_2 levelized cost can be achieved with aggressive R&D targets in locations with excellent resources by 2050.

4.1 PV-MSALT-HTSE can be Cost Competitive with Grid-Electrolysis in the 2020 and 2050 Scenarios

In the 2020 scenario, the grid-electrolysis system has the lowest HLC and the PV-MSALT-HTSE is the solar hydrogen system with the closest HLC. The baseline HLCs for Grid-LTE, PV-LTE, MSALT-HTSE and PV-MSALT-HTSE systems are presented below in Table 17.

Table 17. Baseline System Capacities and Hydrogen Levelized Costs for 2020 and 2050 Scenarios

System	System Capacities	HLC 2020 (2020$/kg H_2)	HLC 2050 (2020$/kg H_2)
Grid-LTE	131 MW LTE	2.82	2.50
PV-LTE	100 MW PV | 55 MW LTE	3.86	2.13
MSALT-HTSE	115 MWe/25 MWth Tower | 130 MW HTSE	3.93	2.84
PV-MSALT-HTSE	100 MW PV | 15 MWth Tower | 60 MW HTSE	2.90	2.15

None of our four systems achieve the $2/kg H_2 HLC in our 2050 scenarios. Section 4.2 will explore capital cost targets that would enable $2/kg H_2 for the solar to hydrogen systems and whether these cost targets align with current R&D projections up to 2050.

In the 2050 scenarios, the PV-LTE and PV-MSALT-HTSE systems have the lowest HLCs due to reductions in assumed PV capital costs from $1.377/Wac to $0.776/Wac, reductions LTE purchase cost assumptions from $342/kW to $143/kW and an improvement in the LTE efficiency from 50.4 kWh/kgH_2 to 47.8 kWh/kgH_2. In the 2050 scenario, both systems have noticeably lower HLCs than the grid-electrolysis system at current-day grid electricity prices. The MSALT-HTSE HLC reduction between the 2020 and 2050 scenarios is primarily due to tower capital cost reductions from $6,577/kW to $4,213/kW. The molten salt tower efficiency is not changed between scenarios because the technology is assumed to be the same. However, there may be value in evaluating the economic impacts of the supercritical CO_2 power cycle design when it is available in SAM.

The PV-MSALT-HTSE system is competitive or the lowest cost hydrogen production system in both the 2020 scenario and 2050 scenario. This supports our initial hypothesis that a hybrid system that utilizes higher efficiency HTSEs, lower cost PV electrons and CSP heat would be competitive with PV-LTE systems. While the PV-MSALT-HTSE in this analysis is sized optimally, it isn't dispatched optimally. Thus, additional work on including battery storage, using a hybrid molten salt tower that provides heat and electricity and hybrid dispatch optimization using a platform such as Hybrid Optimization and Performance Platform (HOPP[2]) could reduce the HLC by further optimizing the performance of the PV-MSALT-HTSE system. As a result, the HLC for the PV-MSALT-HTSE may approach or beat the $2/kg H_2 target in locations with excellent solar resources.

4.2 Parameters needed to meet the $2/kg H_2 HLC Target for the Solar to Hydrogen Systems

Our analysis shows that, of the four systems analyzed, only PV-LTE and PV-MSALT-HTSE approach $2/kg H_2 in high solar resource locations in the 2050 scenario, although the PV-MSALT-HTSE is more competitive than other options in regions with better solar resources. This result is partly due to the concentrating solar system's requirement for direct radiation whereas PV systems more readily capture diffuse irradiation. The following conclusions were also made regarding these two systems.

Trimming Electricity and Heat

For PV-LTE systems (without batteries), the optimal PV:LTE system capacity ratio is 100 MW:55 MW in the current and future scenarios, respectively. At this ratio, negligible amounts of electricity is trimmed (0.2% of the total annual PV generation at Daggett, CA) which indicates that optimally sized PV-LTE systems generally trim little electricity. In the current scenario, when the LTE capacity is reduced by 10 MW below the cost optimal LTE capacity (i.e., the system capacity ratio is 100 MW: 45 MW), significant electricity is trimmed resulting a HLC increase of 6%. When the LTE system is sized 10 MW above the cost optimal LTE capacity (i.e., the system capacity ratio is 100 MW: 65 MW, the increased capital cost of the LTE system results in a HLC increase of 6%. In the future scenario, similar HLC increases are observed with over-sized LTEs but diminished in effect as the cost of additional LTE capacity is cheaper. Sizing an LTE to minimize electricity trimming is cost-optimal but, slightly over or undersized LTEs do not result in considerably higher HLCs.

For PV-MSALT-HTSE systems, optimal system configurations trim little electricity (~5%) and some heat (~20%). Electricity is generally trimmed when solar electricity generation is greater than the nominal HTSE capacity or when there isn't sufficient heat from the heat-only molten salt tower due to

[2] https://github.com/NREL/HOPP

available energy through thermal storage or irradiation. Generally, it is more cost-optimal to trim more heat compared to electricity as the levelized costs of producing heat are lower than electricity.

Lowest Cost Hydrogen Production Systems in the 2020 and 2050 scenarios across the U.S.
Our analysis indicates that PV-LTE systems have lower HLCs compared to PV-MSALT-HTSE systems in most locations in the country in the 2050 scenario; however, in locations with excellent solar resources, the difference between PV-MSALT-HTSE and PV-LTE systems is approximately 1%, which is well within simulation and projection errors. In locations with poorer solar resources such as north-east of the continental U.S., PV-LTE system have up to 22% lower HLCs than PV-MSALT-HTSE systems due to weather conditions generally being unfavorable for concentrating solar relative to photovoltaic systems.

PV-MSALT-HTSE systems have competitive HLCs in excellent solar resource locations in both the 2020 and 2050 scenarios whereas PV-LTE systems have competitive HLCs in excellent solar resource locations only in the 2050 scenario. Because solar-hydrogen systems are more likely to be considered in regions with excellent solar resources and PV-MSALT-HTSE systems are similarly viable to PV-LTE systems in those locations, both are valuable options for future consideration.

Reaching a Hydrogen Levelized Cost of $2/kg H_2

Costs between the moderate and aggressive R&D targets will need to be achieved for all the systems analyzed to meet the $2/kg H_2 target in locations with excellent solar resources such as Daggett, California. Current 2021 ATB projections for utility PV CAPEX in 2050 are 0.481, 0.638, and $0.776/Wac for advanced, moderate and conservative R&D scenarios, respectively. In Daggett, PV costs of $0.68/Wac or moderate ATB PV CAPEX projections result in HLCs of $2/kg H_2. Similarly for PV-MSALT-HTSE systems, $0.60/Wac result in $2/kg H_2 in Daggett, CA which is similar to ATB moderate R&D 2050 projections. For the MSALT-HTSE systems, better than aggressive 2050 ATB salt tower CAPEX projections would be needed to reach $2/kg H_2. In Daggett, molten salt tower capital costs (includes the power block and thermal storage) of $2400/kW would enable $2/kg H_2 in 2050. This is slightly lower than current advanced ATB R&D projections of $2,743/kW in 2050. Outside of Daggett and other excellent solar resource locations, only PV-LTE systems achieve $2/kg H_2 . PV-LTE systems can approach $2/kg H_2 in the Midwest under aggressive ATB R&D scenarios for PV capital costs. Further work on achieving $2/kg H_2 and eventually $1/kg H_2 could be evaluating a combination of improved efficiency or new technologies, hybrid system options (both hydrogen and electricity sales), and optimized dispatch as mentioned in Section 4.1.

4.3 Impact of Batteries on HLCs for PV-LTE Systems

Adding batteries to run smaller LTEs at a higher capacity factor result in lower HLCs than PV-LTE systems without batteries when LTE stack purchase costs are $782/kW and batteries are reduced 90% from current costs as per DOE Earthshot Long Duration Storage Shot targets (“Long Duration Storage Shot: An Introduction” 2021). The HLC is reduced to $3.27/kg H_2 by adding a 50 MW/400 MWh battery to a 25 MW LTE from the $3.73/kg H_2 baseline. All other configurations resulted in negligible HLC cost reductions and no PV-LTE-Battery configuration reaches a HLC $2/kg H_2. For example, at $143/kW LTE purchase costs, the overall HLC is not reduced when batteries are included even with 90% cost reductions in the battery capital cost. A 50 MW/600 MWh battery added to a 30 MW LTE at stack purchase costs of $143/kW is $2.33/kg H_2 or 10% higher than the HLC of the storage-less PV-LTE system. Thus, there is a potential that hydrogen can be produced at $2/kg H_2 at greater than 75 %

capacity factors with further reductions in PV and LTE costs. Because these estimates were developed with only a heuristic-based operational algorithm, a rigorous cost optimization of the battery configuration and dispatch with a demand constraint could realize better results. That analysis could be performed using a platform such as HOPP.

5 References

"2021 Annual Technology Baseline Concentrating Solar Power." 2021. 2021. https://atb.nrel.gov/electricity/2022/concentrating_solar_power.

"2021 Annual Technology Baseline Utility Scale Battery Storage." 2021. 2021. https://atb.nrel.gov/electricity/2022/utility-scale_battery_storage.

"2021 Annual Technology Baseline Utility-Scale PV." 2021. 2021. https://atb.nrel.gov/electricity/2022/utility-scale_pv.

California ISO. 2022. "OASIS." 2022. http://oasis.caiso.com/mrioasis/logon.do.

DiOrio, Nicholas, Aron Dobos, Steven Janzou, Austin Nelson, and Blake Lundstrom. 2015. "Technoeconomic Modeling of Battery Energy Storage in SAM." NREL/TP--6A20-64641, 1225314. https://doi.org/10.2172/1225314.

"DOE Energy Earthshots - Hydrogen Shot." 2021. 2021. https://www.energy.gov/eere/fuelcells/hydrogen-shot.

Gilman, Paul, Nicholas A. DiOrio, Janine M. Freeman, Steven Janzou, Aron Dobos, and David Ryberg. 2018. "SAM Photovoltaic Model Technical Reference 2016 Update." NREL/TP--6A20-67399, 1429291. https://doi.org/10.2172/1429291.

"H2FAST: Hydrogen Financial Analysis Scenario Tool." 2017. October 11, 2017. https://www.nrel.gov/hydrogen/h2fast.html.

James, Brian. 2013. "PEM Electrolysis H2A Production Case Study Documentation." December 31. https://www.nrel.gov/hydrogen/assets/pdfs/h2a-pem-electrolysis-case-study-documentation.pdf.

Kobos, Peter, Anna Lord, David Borns, and Geoffrey Klise. 2011. "A Life Cycle Cost Analysis Framework for Geologic Storage of Hydrogen : A User's Tool." SAND2011-6221, 1029761. https://doi.org/10.2172/1029761.

Kotowicz, Janusz, Daniel Węcel, and Michał Jurczyk. 2018. "Analysis of Component Operation in Power-to-Gas-to-Power Installations." *Applied Energy* 216 (April): 45–59. https://doi.org/10.1016/j.apenergy.2018.02.050.

"Long Duration Storage Shot: An Introduction." 2021. U.S. Department of Energy. https://www.energy.gov/sites/default/files/2021-07/Storage%20shot%20fact%20sheet_071321_%20final.pdf.

"NREL-PySAM 3.0.1." n.d. https://nrel-pysam.readthedocs.io/en/master/.

Pivovar, Bryan, Neha Rustagi, and Sunita Satyapal. 2018. "Hydrogen at Scale (H_2 @Scale): Key to a Clean, Economic, and Sustainable Energy System." *The Electrochemical Society Interface* 27 (1): 47–52. https://doi.org/10.1149/2.F04181if.

Ruth, Mark, Paige Jadun, Nicholas Gilroy, Elizabeth Connelly, Amgad Elgowainy, Richard Boardman, Suzanne Singer, and Jarett Zuboy. 2019. "The Technical and Economic Potential of H2@Scale within the United States." March 1.

Sargent & Lundy LLC Consulting Group, Not Given. 2003. "Assessment of Parabolic Trough and Power Tower Solar Technology Cost and Performance Forecasts." NREL/SR-550-34440, 15005520. https://doi.org/10.2172/15005520.

Turchi, C. S., and G. A. Heath. 2013. "Molten Salt Power Tower Cost Model for the System Advisor Model (SAM)." NREL/TP-5500-57625, 1067902. https://doi.org/10.2172/1067902.

Wendt, Daniel, and Lane Knighton. 2022. "High Temperature Steam Electrolysis Process Performance and Cost Estimates." INL/RPT-22-66117-Rev000, 1867883. https://doi.org/10.2172/1867883.